NOTICE

The quality of this microform is heavily dependent upon the quality of the original thesis submitted for microfilming. Every effort has been made to ensure the highest quality of reproduction possible.

If pages are missing, contact the university which granted the degree.

Some pages may have indistinct print especially if the original pages were typed with a poor typewriter ribbon or if the university sent us an inferior photocopy.

Reproduction in full or in part of this microform is governed by the Canadian Copyright Act, R.S.C. 1970, c. C-30, and subsequent amendments.

AVIS

La qualité de cette microforme dépend grandement de la qualité de la thèse soumise au microfilmage. Nous avons tout fait pour assurer une qualité supérieure de reproduction.

S'il manque des pages, veuillez communiquer avec l'université qui a conféré le grade.

La qualité d'impression de certaines pages peut laisser à désirer, surtout si les pages originales ont été dactylographiées à l'aide d'un ruban usé ou si l'université nous a fait parvenir une photocopie de qualité inférieure.

La reproduction, même partielle, de cette microforme est soumise à la Loi canadienne sur le droit d'auteur, SRC 1970, c. C-30, et ses amendements subséquents.

Canada

PLASMA POLYMERIZED MEMBRANES FOR GAS SEPARATION

By

Marie Therese Sarofeim

A THESIS SUBMITTED TO
THE SCHOOL OF GRADUATE STUDIES AND RESEARCH
IN PARTIAL FULFILLMENT OF THE REQUIREMENTS
FOR THE DEGREE OF
MASTER OF APPLIED SCIENCE
IN THE DEPARTMENT OF CHEMICAL ENGINEERING
UNIVERSITY OF OTTAWA

Ottawa, Ontario,
September 1994

ISBN 0-612-00552-6

UNIVERSITÉ D'OTTAWA
UNIVERSITY OF OTTAWA

Abstract

A plasma-polymerized thin layer was deposited on the top surface of the skin layer of the asymmetric polyethersulfone Victrex (PES) membrane to plug the ultrafine pores. Aniline was used as the monomer gas of plasma polymerization.

Surface characterization by X-ray photoelectron spectroscopy (XPS) measurements has been used to gain insights into the chemistry of plasma-modified membrane surfaces.

The steady-state permeation rates for hydrogen, helium, methane, nitrogen, oxygen and carbon dioxide through the asymmetric PES membranes with the plasma modification were measured to evaluate the permeability and the permselectivity.

The effect of polyaniline plasma and deposition time on the transport properties of plasma deposits are also discussed.

In another set of experiments mixtures of CH_4/CO_2 with known compositions were separated using a laminated PES membrane.

The modified resistance model was employed to analyze the data of PES membranes laminated with a layer of 1.5 mil silicone unbacked rubber.

Acknowledgment

I would like to express my gratitude to Professors T. Matsuura and H. Tezel from University of Ottawa and Dr. M. D. Guiver from the National Research Council for their insight, guidance and assistance throughout the course of this work.

I am also grateful to Dr. A. Fouda, from the National Research Council whose knowledge of computer programming and gas separation expertise was very helpful. I also wish to thank my friends at the Industrial Membrane Research Institute.

I wish to thank Dr. Y. Deslandes from The Environmental Protection Science for the X-ray Photo Electron Spectroscopy analysis.

The financial assistance provided by NSERC is gratefully acknowledged. The availability of the equipment and the technical support provided by the Process Technology section of the National Research Council are also deeply appreciated.

Nomenclature

A_1	area of top layer which is over the substrate's membrane matrix (membrane matrix consists of network pores), m^2
$A_{1'}$	area of top layer which is over the substrate's pores, m^2
A_2	area of substrate membrane matrix of the coating interface (composed of network pores), m^2
A_3	area of the pores on the surface of the substrate membrane, m^2
A_t	total area available for permeation, $A_t = A_2 + A_3 = A_1 + A_{1'}$, m^2
BE	binding energy of emitted electrons (eV.)
hν	energy of x-ray photon (eV.)
KE	kinetic energy of emitted electrons (eV.)
$l_1, l_{1'}$	thickness of top layer of section 1 and 1', m
l_2	effective thickness of substrate membrane, m
l_3	effective thickness of pores (aggregate pores) in substrate membrane, m
$P_{j,i}$	intrinsic permeability of section j for gas i where j = 1,1', 2, 3 and i=N_2, O_2, CO_2, CH_4, $mol.m/m^2.s.Pa$
ΔP	pressure difference across the membrane, Pa
Q_i	permeation rate of component i, mol/s

$(R_j)_i$	resistance of flux for section j for gas i, Pa.s/mol
$(R_t)_i$	total resistance to flux for gas i through the substrate membrane, Pa.s/mol
$(R^L_t)_i$	total resistance to flux for gas i through the laminated membrane, Pa.s/mol

Greek Letters

α_j	$=(R_j)_i/(R_j)CO_2$, ratio of the resistance of gas i flux over the resistance of CO_2 flux for section j
α_t	$=(R_t)_i/(R_t)_{CO2}$ ratio of the total resistance of gas i flux over the total resistance of CO_2 flux for the substrate membrane
α^L_t	$= (R^l_t)_i/(R^l_t)_{CO2}$, total resistance of gas i flux over the total resistance of CO_2 flux for the composite membrane
α	Separation factor defined by equation 21
ν	angular frequency (sec^{-1})
$\emptyset_s$	work function of spectrometer (characteristic of each individual instrument - a constant)

Subscripts

1, 1'	silicone layer, silicone layer above the pores
2	polymer matrix
3	skin layer pores
i,	O_2 or N_2
j	CH_4 or CO_2
t	total

Supercript

L	laminated membrane

Table of Contents

List of Tables

List of Figures

Chapter 1

Introduction

1.1 Historical Overview

For many years, membranes were confined to specific applications, usually as delicate, often expensive, and frequently low volume separation devices.

Gas separation using membranes in industry is a relatively new field even though their potential has been known for some time. Thomas Graham (Stanley, 1986), was the first to realize that various gases possessed different permeation velocities through a membrane. It was not until the early 40's that membranes were used industrially to enrich Uranium 235 (Werner, 1986) from approximately 0.71 % to approximately 3 % by weight, but this method was only employed because there was no alternative process.

It was difficult for the first generation of gas separation membranes to compete with cryogenics and the more highly developed, well entrenched, non membrane processes (Spillman, 1989). The fact that gas membranes achieved the impact they have is a testament to their inherent advantages that include low capital investment, ease of

operation, low energy consumption, cost effectiveness (even at low gas volumes), and good weight and space efficiency (Spillman, 1989).

In the 50's and 60's, small scale experiments on membrane units had been performed at various locations, but there was a lack of membranes with adequately high permeability and separation efficiencies to allow for their use commercially. This problem was solved with the invention of an asymmetrically structured membrane, described by Loeb and Sourirajan (1960). It consists of a very thin, non porous, selective skin layer resting on a highly-porous non selective support layer. The separation of differing components occurs in the skin layer, while the porous substructure provides the mechanical strength for the membrane.

With the development of certain asymmetric membranes by Monsanto (Henis and Tripodi, 1980 a& b), the major stumbling block for gas separation was effectively removed. The basic idea is to have a thin layer of highly permeable, nonselective polymer placed on the surface of the asymmetric membrane. The coating reduces permeability through pores and defects of the asymmetric membrane and allows permeation to occur primarily through the dense skin.

The first commercial gas separation membrane was of a polysulfone material. A tubular hollow-fiber form provided natural mechanical strength and the polysulfone material possessed high chemical resistance. This membrane was introduced to the market in 1979 as the Prism Separator in hydrogen separation from hydrogenation and ammonia production processes.

The composite membranes which have been made by supporting a thin separating membrane on a porous substrate to achieve high fluxes was the latest major innovation and the most economically successful break-through for membranes in gas separation (Henis and Tripodi, 1980).

1.2 Plasma Polymerization

Plasma polymerization or glow discharge polymerization refers to the formation of polymeric materials under the influence of plasma (partially ionized gas) consisting of ions of either polarity, electrons, neutral atoms and molecules in the ground state and in any excited state. It was known for many years that some organic compounds form solid deposit in plasma generated by some kinds of electric discharge (Schoepfle and Connell, 1929; Austin and Black, 1930; Linder and Davis, 1931; Harkins and Jackson, 1933; Otazai et al, 1954; Weisz, 1955). In most cases, however, the polymers were recognized as byproducts of phenomena associated with electric discharge; consequently, little attention was paid either to properties of these polymers (undesirable byproducts) or to the process as a means of forming useful polymers.

Only since the 1960's has the formation of materials in plasma been recognized as a means of synthesizing polymers, and the process, when used to make a special coating on metals, has been referred to as polymerization or glow discharge polymerization (Goodman, 1960; Arquette, 1962; Coleman, 1962; Stuart, 1963; Bradley and Hammes, 1963).

In more recent years, however, the question of whether or not the concepts of polymers and polymerization can be applied to plasma-formed materials and to plasma polymerization, respectively, has been reexamined by Yasuda (1979). The well-recognized concept of polymerization today is based on the molecular process by which the size of molecule increases. The arrangement of the atoms that constitute the molecules of a monomer is accomplished during the organic synthesis of the monomer. During the polymerization of a monomer, rearrangement of atoms within the molecules seldom occurs.

In contrast to such a molecular processes, polymer formation in plasma has been recognized as an atomic (non molecular) process (Yasuda, 1979). If one adopted such an atomic process to form materials in which the reaction of new covalent bonds between atoms played a predominant role, one could find numerous new processes and resulting materials that would play vitally important roles in modern technologies. The processes recognized as chemical vapor deposition, plasma chemical vapor deposition, ion-assisted vapor deposition and sputter coating of polymers all fall into this category.

Plasma polymerization was used between 1960 and 1970 as a method of polymerization. Although some important differences in polymer formation mechanisms and the properties of resultant polymers were recognized, the underlying concepts of polymerization and polymers were developed with conventional polymers.

Today Plasma polymerization is gaining recognition as an important process for the formation of entirely new kinds of materials. The principal application of plasma polymer films may be conveniently divided into two classes. The first involves the alteration of the surface properties of a substrate. An example of such an application includes the modification of a polymer surface for the purpose of increasing (or decreasing) adhesion of the interface. Secondly, the application may capitalize on the bulk properties of a thin, pinhole free, and highly adherent film. An example would be the use of the transport properties of such films as in permselective membranes for gas purification.

1.3. Applications Based on Plasma Polymer Bulk Properties

1.3.1 Material Transport Through Plasma Polymers

The ease with which extremely thin and integral films can be deposited suggests their use for separation processes based on preferential transport through the membrane, of one component of a mixture. The flux of such diffusive transport will be inversely proportional to the thickness of the membrane, hence the inherent appeal of plasma polymer films. Several examples exist in the survey of the applications of such films for gas separation, ultrafiltration, pervaporation and reverse osmosis.

It is well known that plasma polymerization is a suitable method for the preparation of thin and pinhole free films that adhere well to the substrates. Saruyama (1991), has demonstrated that plasma polymerization of hexamethyl disiloxane using porous polypropylene as a substrate leads to a useful film with oxygen permeability of $5x10^{-5}$ $cm^3/cm^2.s.cm.Hg$ vs. oxygen permeability of $1x10^{-5}$ without siloxane. Various flexible substrates have been coated with polymer films using nitrogen containing monomers (Kawakami et al., 1984); the resulting plasma polymers were studied for their application in O_2/N_2 separations. Coatings of 4-vinyl pyridine, 2-vinyl pyridine and perfluro tri-n-butylamine plasma polymers were found to be effective in increasing the O_2/N_2 permeability ratios of natural rubber (3.1) and polydimethylsiloxane (3.4) respectively, but not for polyurethane or an aromatic polysulfone. It was noted that the first two monomers form conventional polymers that have a high permeability ratio of O_2 to N_2 but are brittle. The advantage of plasma polymerization is that a thin, robust permselective membrane may be formed, the enhanced separation being caused presumably by the increased solubility of oxygen in the deposited layer.

The most systematic study of plasma polymer permselectivity to date was done by Nomura et al. (1984) in which the selectivity for H_2/CO_2 was 16. This work identifies larger monomer size as conducive to effective permselectivity. The greater permeability ratios attainable for separations based on molecular size (H_2/N_2, H_2/CO_2, He/CO_2) than on solubility (O_2/N_2 and CO_2/CH_4) are also noted. The selectivity of O_2/N_2 was 1.95 at a coating thickness of 2500 Å.

The importance of pore size in porous substrates was demonstrated by Canepa et al. (1984) and Sakata et al. (1986). In the later work (Sakata et al., 1986), the monomers, tetramethylsilane, hexamethyldisiloxane, and octamethylcylotetrasiloxane, were plasma polymerized onto a porous Celgard. It was found that selectivity (O_2/N_2) for plasma polymer deposited on porous Celgard was nil below a coating thickness of 1600 Å, but reached a plateau for greater thickness (indicating coverage of all pores). The higher permeselectivity was obtained for plasma polymers derived from the lower molecular weight monomers in contradiction of the trend found by Nomura et al. (1984).

The transport of water through plasma polymers, with exclusion of ions, has been studied with a view to using these thin films for reverse osmosis purification of saline and waste water (Hollahan, 1977; Yasuda et al., 1976).

Stancell and Spencer (1972) investigated the gas permeabilities of composite films prepared by the deposition of plasma polymers from a number of starting monomers on silicone-carbonate (SC) copolymer film. The monomers were divided into three groups based on their chemical structures: nitrile, vinyl and aromatic types. The composite membranes prepared from plasma polymers of the nitrile-type monomers had the highest permeability ratios of hydrogen to methane (37), followed by the vinyl-type plasma polymers and then the plasma polymers from the aromatic compounds.

Chang et al. (1973) studied the effect of plasma polymerized ethylene deposited on poly(dimethylsiloxane) on oxygen permeability as a function of treatment time. The oxygen permeability coefficients decrease with increasing treatment time, due to the increase of plasma polymer coating thickness for the ethylene plasma polymer deposition. The deposition of plasma polymer coatings is more effective in decreasing the oxygen permeation than an argon plasma treatment.

The Plasma-Graft technique has been applied in the preparation of a pervaporation membrane by Hirotsu and Nakajma (1988). The membrane consists of porous polypropylene film as the substrate and a hydrophilic grafted layer such as poly(acrylic acid), and poly(methacrylic acid). These membranes exhibited water permselectivities for water/ethanol mixtures. They reported that the hydrophilic grafted layers were mainly formed on the surface of the substrates (Hirotsu and Isayama, 1989). A new technique called plasma-Graft filling polymerization was proposed by Yamaguchi et al. (1991) and applied in the synthesis of a new organic membrane used for liquid separation. It was called the filling polymerized membrane. Two kinds of porous substrates, high density polyethylene (HDPE) films and high density polyethylene and poly(methylacrylate), were used as the grafted polymers. The grafted layers filled the substrate pores. These membranes showed high permselectivity for benzene and the filling polymerized membrane swelling raised the selectivity.

Table 1 is the summary of the literature survey on detailed plasma membranes information with references covered by Chemical Abstracts for the period 1967-present. Some of the information listed here are for different supports and films. Commonly used supports for plasma are polypropylene (Saruyama, 1991; Hirotus and Arita, 1991; Hirotu and Isayama, 1989; Sakata et al., 1989; Hirotsu and Nakajima, 1988; Sakata, 1988; Kashiwagi et al., 1987; Hirotsus et al., 1987; Hasumi et al., 1987) and polysulphone

(Sada et al., 1990; Kramer and Yasuda, 1988; Masuoka et.al., 1987; Samejiima and Nakamura, 1987; Masuoka and Mizoguchi, 1987; Kramer and Yasuda, 1987; Wolff et al., 1986; Okita, 1985; Nomura, Kramer, and Yasuda, 1984).

Some plasma deposited films are from flurocarbon compounds (Sada et al, 1990; Inagaki, 1987), vinylpyridines (Saruyama, 1991; Okita et al., 1986; Kawakami et al., 1984), siloxanes (Saruyama, 1991; Hirota and Nakabo, 1991; Cai et al., 1989; Sakata et al., 1989; Sakata et al., 1988; Kashiwagi, et al., 1988; Koichi and Sigeru, 1983), acrylic compounds (Yamaguchi et al., 1991; Hirotsu, Najima, 1988; Hirotsu, 1987) and miscellaneous (Kasiwagi, Okabe, 1987; Canepa, Nicchia, Munari and Bena, 1984; Heffernan et al., 1984).

Table 1: Material Transport through Plasma Polymers

STN#	Polym.	Material Substrate	Material	Conditions	Membrane	Application	Reference
2	P	porous polypropylene	hexamethyldisiloxane		GAS	oxygen enrichment; 5 x 10-5 cm3/cm2 .s. cm. Hg vs. 10-5 without siloxane	Jpn. Kokai Tokkyo Koho, JP 03101818; 26 Apr 1991
3	F	porous polypropylene	4-vinylpyridine	288 K; 0.1 Torr; treated with Benzylchloride; Ar. 20 minutes	UF (ultrafiltration)		Jpn. Kokai Tokkyo Koho, JP 03086730; 11 Apr 1991
4	F	porous high-d polyethylene	Me acrylate	13.5 MHz, 10 W			Macro molecules; 24 (20), 5522-7 (1991)
5	F	polyethylene	polyethylene glycol dimethacrylate	0.1 torr; 100 W; treated area; Ar 100 cm2	UF	imparting antithrombic properties and stain resistance.	Eur. Pat.; Appl., EP 424873; May 1991
8	P	polyacetylene with silyl or germyl groups	poly (trimethylsilylpropyne)	0.1 - 0.4 torr.; Ar; 200W; 25-50 mtorr.; 20 min.	GAS	O permeability; N permeability	US. patent US 5013338, 7 May 1991
9	P	porous Duragard 2400	PTFE and poly (4methyl-1-pentene)	Ar. gas; 13.56 MHz; 10W	GAS	separation of oxygen	Jpn. Kokai Tokkyo Koho, JP 03042021; 22 Feb. 1991
10	P	porous Duragard	hexamethyl disiloxane & poly (4-methyl-1-pentene)	Ar gas; 13.56 MHz; 10W	GAS	separation of oxygen	Jpn. Kokai Tokkyo Koho, JP 03042022 ; 22 Feb. 1991
11	F	porous polypropylene;	N,N-dimethylaminoethyl methacrylate grafted		PERVAP	pervaporation of water-ETOH	J. Appl. Polym. Sci., 42 (12), 3255-61 (1991)
12	P	porous Duragard 2400	dimethyl siloxane; + poly (4methyl-1-pentene)	13.56 MHz; 10W	GAS	separation of oxygen	Jpn. Kokai Tokkyo Koho, JP 03042020A2; 22 Feb. 1991

Table 1: Material Transport through Plasma Polymers

STN#	Polym.	Material Substrate	Material	Conditions	Membrane	Application	Reference
22	P	polysulfone	CHF3		GAS	O2-N2 separation; plug the ultrafine;	J. Appl. Poly. Science; 41 (9-10), 242-7-36 (1990)
24	P	porous inorganic membrane	Ti(PrO4) and MeSiCl3	≤ 0.1 torr; Ar.; pore diameter; 10-50Å	GAS	RO	Jpn. Kokai Tokkyo Koho, JP 0200 9730; 12 Jan. 1990
26	P	arom. polysulphones or arom. polyethersulphones	Ne, Ar, Kr, Xe	10~200 W.; 10S~10 min	GAS	O2-N2 separation	Jpn. Kokai Tokkyo Koho, JP 02071826; 12 March 1990
29	P	hexafluroethaneallyl amine	allylamine with hexafluroethane		PERVAP	separation of ethanol water	Kagaku Kogaku; Ronbunshu,; 16(3), 447-53 (1990)
33	P	di-Me silicone rubber	Siloxanes: hexamethylsiloxane; hexamethylcyclotrisiloxane; octaethylcyclotetrasiloxane; tetramethyl-1,3 bis(hydroxybutyl) disloxane; tetramethyl-1,3-bis (chloromethyl) disiloxane; tetramethyl-1,3-		GAS	O separation N separation	Mo Kexue Yu; Jishu, 9(3), 8-11 (1989)
37	P	Silicone rubber	methane		GAS		J. Appl. Polym.; Sci., 39(7), 1541-52 (1990)
39	F	Celgard 2500 (porous film)	grafted with acrylic acid at room temp. for 2 hours. then with 4-vinylpyridine for 8 h.	13.56 MHz; 60 s. grafted at room temp. for 2 hours. 0.02 torr	PERVAP		Jpn. Kokai Tokkyo Koho, JP 07275639; 6 Nov. 1989

Table 1: Material Transport through Plasma Polymers

STN#	Polym.	Material Substrate	Material	Conditions	Membrane	Application	Reference
42	F	porous celgard; polypropylene II	graft; CH2=C(CH3)COO(CH2)2OH (I) then graft polymer of acrylamide (II) onto film	Min. amount (I) to fill pores:1.5 mg/cm2 and <0.5 mg/cm2 for the membranes formed	PERVAP	water ethanol. separation	Proc. Int. Conf. Pervaporation Process Chem. Ind., 3rd, 103-9 Edited by Batish Robert A Bakish Mater Corp: Englewood, N.J. (1988)
43	F	porous polypropylene	graft; 2-hydroxylmethacrylate (I)with acrylic acid (II) or methacrylic acid (III) in		PERVAP	water ethanol separation	J. Membrane Sciences,; 45 (1-2), 137-54 (1989)
45	P	perfluoro-2-butyltetrahydrofuran or perfluorobenzene	CH4 CF4 mixtures		GAS	O separation; N separation	Proc. Jpn. Symp. Plasma Chem., 1, 297-302 (1988)
47	P	fluoroalkylacrylates and methacrylates			GAS	O separation; N separation	Polym. Bull (Berlin),; 21(4), 371-6 (1989)
50	P	porous propylene	1st layer; hexamethyl disiloxane; 2nd layer; 1-hexene, cyclohexene,; toluene, benzene, styrene; divinylbenzene, 1,3 pentadiene; 1,3-cyclodiene, acetylene, 1-heptyene, acrylic acid, Et-acrylate, acetylenecarboxylic acid,		GAS	H separation; N separation	J. Appl. Polym. Sci., 37(9), 2773-9 (1989)
55	F	porous Duragard	graft with acrylamide (I) and then hydroxymethylated with paraformaldehyde			water alcohol separation	Jpn. Kokai Tokkyo Koho, JP 0103062; 1 Feb. 1989
59	P		1-(trimethylsilyl)-1-propyne		GAS	He, H, O, N, CO2 and CH4	polym. bull.; (Berlin), 20(4); 349-54 (1988)

Table 1: Material Transport through Plasma Polymers

S'r N#	Polym.	Material Substrate	Material	Conditions	Membrane	Application	Reference
61	F; P	hexamethyldisloxane I	dimethylsiloxane chains with branches of trimethylsilyl groups then the films deposited from I Nucleopore	reaction chamber had the triode electrode surface energy of the film	PERVAP	ethanol-water separation	Desalination,; 70 (1-3), 465-79 (1988)
62	P	porous Udel P1700; support	alkylenediamines (ethylenediamine) 0.09; epichlorohydrin 0.06, and glutaraldehyde (1) 0.005 mol. under plasma.		RO	water permeability	Jpn. Kokai Tokkyo Koho, JP 63134006; 6 June 1988
67	P	porous polysulphone	perflurodimethylcyclobutane	electrodes (clean or preconditioned)	GAS	air separation	J. Appl. Polym. Sci.; Appl. Poly. Symp., (vol. date1987); 42 (plasma polym. plasma treat. polym.); 381-409 (1988)
68	P		CF4 perfluorobenzene and from mix. of		GAS	O separation; N separation	J. Membr. Sci., 38(1), 85-95 (1988)
69	P		CF4 and hexafluropropylene with Me4Si vinyltrimethysilane or ethyltrimethysiloxane		GAS	O separation	J. Appl. Polym. Sci; Appl. Polym Symp; (vol. date 1987), 42 (Plasma polym. plasma treat. polym.) 327-38 (1988)
70	P	porous substrate	hexamethyldisiloxane and octamethylcyclotetrasiloxane		GAS	O separation; N separation	Kobushi Ronbunshu, 45(6), 499-503 (1988)
71	P	porous glass hollow fibers	hexamethyldisiloxane	plasma polymn. was performed 4 times; air blowing was carried out between plasma polymn.	GAS	oxygen enrichment	J. Appl. Polym. Sci.; Appl. Polym. Symp., (vol. Date 1987); 42 (plasma polym.; plasma treat. polym); 339-56 (1988)
73	F	porous propylene	graft acrylic acid with acrylamide		PERVAP	water ethanol permseparation	J. Appl. Polym Sci., 36 (1), 177-89 (1988)

Table 1: Material Transport through Plasma Polymers

ST N#	Polym.	Material Substrate	Material	Conditions	Membrane	Application	Reference
74	F		hexamethyldisiloxane followed by plasma polym. of perfluorobenzene		GAS		Kita Kyushu Kogyo; Koto. Semmon; Gakko Kenkyu; Hokoku, 21, 45-50
75	P (F)	hydrophobic porous membrane Duragard 2400	1,1,1,3,5,5,5-heptamethyltrisiloxane in the presence of O plasma, resulting product impreg. onto		PERVAP	ETOH-H2O separation	Jpn. Kokai Tokkyo Koho, JP 63044903; 25 Feb. 1988
76	P	porous polycarbonate or propylene	hexamethyldisiloxane	radius of pores of the substate 110 or 230Å	GAS		Maku, 13(1); 45-50 (1988)
77	P	Duragard 2400 (propylene)	(Me3Si)2O in the presence of Ar and O		PERVAP	ETOH-H2O separation	Jpn. Kokai Tokkyo Koho, JP 62225209; Oct. 1987
78	P	porous polysulphone	N plasma and then polymg. furfuryl alc. in aq. H2SO4 to form thin sulphonated polymer layer then immersed in B(6H2) soln for 15 min. washed	low temp. polysulphone pretreated with Nadodecylsulphate instead of N plasma	RO	salt rejection	Jpn. Kokai Tokkyo Koho, JP 62262711; 15 Nov. 1987
79	P	porous polysulphone	gas mixt contg.; C2F6 and allylamine under plasma		PERVAP	EtOH-H2O separation	Jpn. Kokai Tokkyo Koho, JP 62210008; 16 Sept. 1986
80	P	porous fluoroprene FP 010	poly (4 vinylpyridine) and impregnated with a soln of XXX in DMSO		GAS	O separation; N separation	Jpn. Kokai Tokkyo Koho, JP 61293525; 25 Dec. 1986
81	P	1- hydrophobic (Fluoropore FP65); 2- hydrophillic (Fuji	1- org. silicone compound; 2-N gas at	N gas was carried at 2.25 L/min	PERVAP	ETOH-H2O separation	Jpn. Kokai Tokkyo Koho, JP 6222507; 30 Oct. 1987

Table 1: Material Transport through Plasma Polymers

STN#	Polym.	Material Substrate	Material	Conditions	Membrane	Application	Reference
82	P	porous polysulphone	tetrakis (trifluoromethyl) dithietane	av. membrane pore size 30Å; 0.3 torr; 13.56 MHz; membrane layer	GAS	separation of helium from natural gas	Jpn. Kokai Tokkyo Koho, JP 622048526; 9 Sept. 1987
83	P	porous polysulphone	(F3C)2C=C(CF3)2	membrane pore size 30Å; 0.4 torr; 13.56 MHz; membrane layer 1.24	GAS	He separation; N separation	Jpn. Kokai Tokkyo Koho,. JP 62204825; 9 Sept. 1987
84	P	hexamethyldisiloxane	porous glass hollow fiber		GAS	O separtion; N separation	J. Appl. Polym. Sci., 34(8), 2701-11 (1987)
85	P	microporous polypropylene hollow fibre	C3H6	membrane inner diameter 240 µm, wall thickness 24.5 µm; 220 mtorr; 40 W; 5.0 KHz	UF	hydrophobic ultrafiltration	Ger. often, 19 pp.; DE 3712490; 15 Oct. 1987
86	P		tetramethylsilane, trimethylvinylsilane, ethylnythrimethyl silane with		GAS		J. Membr. Sci., 34 (3) 297-305 (1987)
87	P	composite membrane porous asym. anode Al oxide	film is applied by plasma polym., interfacial polym., or by Langmiuir-Blodget Technique		RO, PERVAP; GAS;	air separation, biogas separation.	Eur. Pat. Appl.,; 10 pp.; EP 242209; 21 Oct. 1987
89	P	polysulphone	hexafluoroethane and allylamine	average diameter of the pin hole 0.1-0.45 µm	PERVAP	ETOH-Water separation	Kagaku Kogyo, 38(10), 851-7 (1987)
90	P	Millipore filter	perfluoroalyph. compds and silanes RR"SiR2R3; (R,R1,R2,R3 =H, alkyl,; vinyl, ethynyl); Si Me4 and CF4	13.56MHZ; 50W.; 1.3p.; SiMe4 and CF4; 4:1	GAS	oxygen separation; N separation	Jpn. Kokai Tokkyo Koho, JP 62116776; 28 May 1987

Table 1: Material Transport through Plasma Polymers

STN#	Polym.	Material Substrate	Material	Conditions	Membrane	Application	Reference
91	P,F	porous polypropylene	plasma treated with N2; then grafted with aq. acrylamide	0.001 torr; 10 W; 30 s.	PERVAP	ETOH-H2O separation	Jpn. Kokai Tokkyo Koho, JP 62129112; 11 June 1987
93	F	porous propylene	plasma graft polym. of acrylic acid I; methacrylic acid II; or		PERVAP	water ethanol separation	J. Appl. Polym Sci.,; 34 (3), 1159-72 (1987)
94	P	polyethylene hollow fibre	CH4 plasma then O2 plasma	1 torr for 10 s.; then 0.01 torr for 5 s.	UF		Jpn. Kokai Tokkyo Koho, JP 62083007; 16 Apr. 1987
95	P	Multipore filters	fluorocarbons and silanes		GAS	oxygen separation	Polym. Mater. Sci. Eng., 56,; 797-801 (1987)
98	P	polysulfone hollow fibers	hexafluorobenzene		GAS	N1+, CO2, O and CH4 separation	Kitakyushu Kogyo Koto Sen mom Gakko; Ken Kyu Hokoku; 20,83-9 (1987)
99	P	porous polysulphone	polyperfluorobenzene	RF plasma 40W	GAS		Polym. Mater. Sci. Eng. 56, 807-11 (1987)
101	P	silicone rubber	styrene-vinyl acetate; hexamethyldisiloxane Me		GAS	CO2, CH4 separation	Polym. Mater. Sci. Eng., 56; 792-6
102	P	porous polypropylene	plasma in styrene	0.9-1.1 torr; 13.56 MHz	GAS	O separation; N separation	Jpn. Kokai Tokkyo Koho, JP 62019206; 28 Jan 1987
103	P	porous polysulphone	poly (perfluorodimethylcyclobutane		GAS	O separation; N separation	Polym. Mater. Sci. Eng., 56, 812-16 (1987)
104	P		poly(chlorotrifluroethylene); tetrafluoroethylene hexafluoropropene polymer; then sep. d. using perfluoro-3,6-dioxa-5 methyl-1-nonemetetrafluoroethylene		GAS; PERVAP	oxygen separation; water-ETOH separation	Kogaku Kogyo,; 38(2), 158-63 (1987)

Table 1: Material Transport through Plasma Polymers

STN#	Polym.	Material Substrate	Material	Conditions	Membrane	Application	Reference
105	P	natural rubber; dimethylsiloxane,; polyurethane, arom. polysulfone	4- vinylpyridine		GAS	N separation; O separation	Vysokomol. Soedin., Ser.B,; 29(2), 118-21
107	P		perfluoromethylcyclohexamel; methane		GAS	O separation; N separation	J. Polym. Sci., Part A: Polym. Chem., 24 (12), 3381-91 (12986)
108	P	porous polysulfone asym.	plasma in NH3, swollen 3h in 10% aq caprolactam, then add of 4% halopyrimidine then add reactive diazo dye	730V; 0.29 W/cm3; 0.6 mbar	UF		Ger. Offen., DE 3509068; 18 Sept. 1986
110	P	millipore filter	perfluoromethylcyclolexane and CH4 7:3		GAS	O separation; N separation	Jpn. Kokai Tokkyo Koho, JP 61101207; 20 May 1986
111	P	PTFE	4-vinylpyridine	0.01-0.2 torr; 30 min; 30 W.	GAS	O2 separation; CO separation	Eur. Pat. Appl. EP 186182; 2 Jul. 1986
113	P	fluoropore FP-010; pore size 0.1 μm	4-vinylpyridine		GAS	O enriched	Eur. Pat. Appl. EP. 176986; 9 April 1986
114	P	porous polypropylene	4-vinyl pyridine 70, styrene 20, divinylbenzene 10, PVC powder 60 and benzoyl peroxide, treated with 1:1 MeI-methanol solvent & 2:1		PERVAP		Jpn. Kokai Tokkyo Koho, JP 61061840 A2; 29Mar 1986
116	P	hollow polyethylene	low temp plasma in O then treated with a low temp. plasma in Ar.	5 s. 5OW; 0.01 torr.then 5 s. 0.01 torr; 50W.	UF	water permeation	Jpn. Kokai Tokkyo Koho, JP 61086908; 2 May 1986
119	P	porous polypropylene	hexamethydisilotane and octamethylcyclotetrasiloxane	13.56 MHz; 80W; treatment time 15 min.	UF	H separation	Kitakyushu Kogyo Koto Semon Gakko Kenkyu Hokoku, 19, 101-7 (1986)

Table 1: Material Transport through Plasma Polymers

STN#	Polym.	Material Substrate	Material	Conditions	Membrane	Application	Reference
121	P	porous propylene	tetramethylsilane (TMS); hexamethyldisiloxane (M2) and		GAS	O permeation	J. Appl. polym. Sci., 31(7) 1999-2006 (1986)
123	P	polyarylsulphone	trimethylvinylsilane	0.3 torr.; Glow disharge 20W	GAS	O separation; N separation	Jpn. Kokai Tokkyo Koho, JP 60261528; 24 Dec 1985
124	P	alkynylsilane polymers	low temp. plasma in N. at 0.2 mm		GAS	O	Jpn. Kokai Tokkyo Koho, JP 60232205; 18 Nov 1985
125	P	1- porous support e.g. siloxane polymer or PTFE; 2- porous	1- organosilane then chargang 20cm3/m methyltrivinylsilane vapor	10W 20 min.	GAS	separation of natural gas or air	Jpn. Kokai Tokkyo Koho, JP 60143815; 24 Dec 1985
131	P	porous hollow glass fiber	hexamethyldisiloxane I then with a mixt of I at decreasing conc. and diallydimethylsilane at increasing concn	0.1 torr 2min	GAS	O separation; N separation	Jpn. Kokai Tokkyo Koho, JP 60137417; 22 Jul. 1985
132	P	porous PTFE; (mean pore diam. 0.45 μm)	fluoropore FP045 [9002-840]; impregnated with dimethylsiloxane in MEK; membrane exposed to a plasma; 4-methyl-1-pentene	13.56 MHz and 0.2 torr.	GAS	O separation; N separation	U.S patent US 4533369; 6 Aug. 1985
135	P	porous polysulphone; pore size 30Å	CF2:CFOCF2CF(CF3)OC3F7	0.2 torr; 13.56 MHz; 50W; 1 min.	GAS	He separation; CO2 separation; N separation	Jpn. Kokai Tokkyo Koho, JP 60099323; 3 June 1985
137	P	porous polysulphone	C6F6.	0.4 torr; 13.56 mHz	GAS	He separation; CO2 separation; N separation	Jpn. Kokai Tokkyo Koho, JP 60099324; 3 June 1985

Table 1: Material Transport through Plasma Polymers

ST N#	Polym.	Material Substrate	Material	Conditions	Membrane	Application	Reference
138	P	porous polysulphone	perflurocyclohexene	0.07 torr; 13.56 MHz; 20W. 1 min.	GAS	He separation; CO2 Separation; N separation	Jpn. Kokai Tokkyo Koho, JP 60099325; 3 June 1985
140	P	porous Fluoropore FP022; [9002-84-0]; 0.22 μm pore diam.	20% soln. of SE 955U; (Ph group-contg. silicone rubber) plasma treated 5 min., and laminated with 0.26 μm poly(methyltrivinylsilane)		GAS	O separation; N separation; H separation; CO separation	Jpn. Kokai Tokkyo Koho, JP 60075320; 27 Apr. 1985
142	P	porous polycarbonate; (av.	600 ml Ar/min and 600 ml PhCF3; gas/min	13.56 MHz	GAS	O separation; H2O separation	Jpn. Kokai Tokkyo Koho, JP 60051505; 23 March 1985
143	P	microporous polypropylene; [9003-07-0]	equalvols of dichlorofuromethane and Ar. room temp. then intermediate layer of di-Me siloxamene		GAS	CO2 separation; CH4 separation	Eur. pat. appl., EP 134055; 13 March 1985
146	P	Millipore VSWP; [74565-43-8); pore size 0.025 μm	R3SiC:CSiR3 (I), (R,R1=alkyl, vinyl, alkyl, Ph; or (RC:CSiR2)O (II), (R,R1=M,	0.2 m bar 20 W for 40 min.	GAS	N separation; O separation	Jpn. Kokai Tokkyo Koho, JP 59169507; 25 Sept. 1984
147	P	porous polysulphone	fluorolefins (eg. perfluro-2-butyltetrahydrofuran or pentafluorostyrene)		GAS	separation of binary gas mixts.	Thin solids films, 118 (2), 187-95 (1984)
148	P	porous propylene	rf polyethane [36427-13-1]		GAS		Chim. Ind. (Milan), 6 6(10), 604-7 (1984)
151	P	porous polypropylene; 25 μm, soaked in 3% silicone RTV KE-45	Me3SiCl	0.2 torr; 13.56 MHz	GAS	O separation; N separation	Jpn. Kokai Tokkyo Koho, JP 59069105; 19 April 1984

Table 1: Material Transport through Plasma Polymers

ST N#	Polym.	Material Substrate	Material	Conditions	Membrane	Application	Reference
152	P	porous polyacrylonitrile; [25014-41-9]	non plasma polymerizable gases		RO	high water flux; high salt rejection	J. Appl. Polym. Sci.; Appl. Polym. Symp., 38 (plasma polym. Plasma treat.), 173-83 (1984)
153	P	microporous Nucleopore or Celgard film; pore diam 500Å and narrow pore size	rf plasma of naphthalene		GAS	He separation; H separation; CH4 separation	Chim. Ind. (Milan), 66(4), 238 - 43 (1984)
154	P	natural rubber, poly (dimethylsiloxane); arom. polysulphone, adipic acid diethylene glycol; TDI copolymer	4 vinylpridine and 1-vinylimidazole [1072-63-5]		GAS	O separation; N separation	J. Membr. Sci., 19 (3), 249-58 (1984)
163	P	hollow fibre polysulphone	pyridine or allylamine		RO		Ind. Eng. Chem. Prod. Res. Dev., 23 (1), 153-162 (1984)
164	P	porous polytetrafluoroethylene 0.22 μm	20% soln. dimethylsiloxane in toluene contg. a vulcanizing agent		GAS	O separation; N separation	Eur. Pat. Appl., EP 92417; 26 Oct. 1983
170	P	hollow fiber consisting of posylphone; polyacrylonchile or a copolymer or 89:11 acrylonitrile-vinyl	Me4SiO		GAS	concentrate oxygen in air	Brit. U.K. Pat; Appl,; G.B. 2089285 23 June 1982
171	P	3 nitrile monomers, 3 vinyl monomers, 4 aromatic monomers		350 KHz 100 W	Gas	separation of H2/CH4 butene-1/isobutene	J. App l. Polym. Sci. 16, 1505

Table 1: Material Transport through Plasma Polymers

STN#	Polym.	Material Substrate	Material	Conditions	Membrane	Application	Reference
172	P	Acetylene/H2O/N2			RO	purification of waste water	J. Appl. Pollym. Sci. , 20 , 543-55 (1976)
173	P	porous asymmetric cellulose acetate nitrate (CA-CN)	3-butenenitrile, propyleneimine, 4-vinylpyridine and allyamine		RO	purification of saline and waste water	J. Appl. Polym. Sci. 17,2915 (1973)

1.4 Economics of Gas Separation Membranes

The gas separation membrane industry is still young, new products and processes are constantly appearing. A clearer understanding of new membranes and how their performance affects process economics is slowly emerging.

Throughout the 1970's much research and early developmental work was conducted on gas separation, and out of these efforts many potential applications were identified. Two small companies, Envirogenics and Separex, pioneered work on gas separation, but their small size greatly inhibited successful commercialization. Du Pont also developed and tested membranes for industrial applications in 1970, but commercialization lagged. In 1979 Monsanto introduced a hollow fiber gas membrane (Prism) and began an aggressive marketing effort.

Du Pont suggests that the world present market for gas separation systems can be expected to grow by $1.5 billion by 1995 (Haggin, 1988). This would include several major areas of opportunity such as a market for air separation by membrane systems that could total $600 million by 1995. Principal applications would be enriched air for combustion and high-purity nitrogen for blanketing and use as an inert medium.

A second area of opportunity would be separating carbon dioxide from natural gas. The two major applications in this area would be sweetening pipeline gas and recovering carbon dioxide for reinjection in tertiary oil recovery. This market could increase by as much as $100 million by 1995. The largest market for membrane gas separations is in recovery of hydrogen from process streams in refineries and chemical plants.

The world demand for hydrogen could double by the year 2000 and the demand for hydrogen separation systems could provide a market of $800 million

annually, as suggested by a representative of Du Pont (Haggin, 1988). Several joint ventures have been announced. For example, Du Pont has numerous joint venture arrangements. They include a joint operation with Memtek Corp. of Billerica, Mass, to develop membrane-based gas separation technology to remove toxic organic materials from hazardous aqueous wastes. Another is with FMC. Corp., to develop membrane-based food processing techniques. Of most interest to producers of gas separation systems is a joint venture between Du Pont and Air Liquid to develop, manufacture, and market gas separation systems based on polymeric membrane technology. Early in May 1988, Air Products & Chemicals and Akzo of the Netherlands announced a joint venture to develop membranes for air separation. Also Dow chemical agreed to form a joint venture with U.K.'s BOC to develop capabilities in membrane air separation systems. They will manufacture and sell non-cryogenically produced oxygen and nitrogen using BOC's pressure swing engineering techniques and Dow's hollow fiber membrane technology. Finally, among recent moves, Hoechst Celanese formed a new separations product division to promote the company's membrane systems, which are devoted primarily to health care, food processing, waste changes in the way that technology is developed and applied.

1.5 Transport Mechanisms

Membrane separation processes are based on the selective transport of solution components through a physical barrier. The principal objective of gas separation is to split a feed stream of mixed gases into its constituents. Ideally, both high flux (permeability or throughput) and high selectivity should be obtained, but in practice, the two factors are mutually exclusive with few exceptions (McHattie, 1990).

Gas separation membranes can be rationally designed by understanding the gas separation mechanism, the role of penetrant-membrane interactions and the function of the polymer matrix. A convenient method of classifying membrane transport mechanics is based on the effective pore sizes of the membrane. Figure 1 is a summary of several transport mechanisms currently recognized.

When the pore size is large, (relative to the mean free path) viscous flow involving both convective and diffusive mass transfer predominates (Figure 1 a). Significant gas phase separation is not observed if this is the transport mechanism through a membrane. As the pore size decreases, there is less space for the gas molecules to move about freely. When the pore diameter is less than the mean free path of the gas molecule (50-100 Å), the process of Knudsen diffusion occurs (Figure 1.b). Molecules will collide more frequently with the pore walls than with the gas molecules. In such cases, permeability through the membrane is inversely proportional to the molecular weight of the component gases and a small separation factor can be obtained for gases with large molecular weight differences.

A separation mechanism based on molecular sieving can occur when the pore size is reduced to the order of individual gas molecules (less than 7 Å) (Figure 1.c). Zeolites are examples of naturally occurring molecular sieves. Separation or selectivity is generally good but the permeability is very low since the pores are highly tortuous.

When the effective pore size is described by the intermolecular spaces between the polymer chains within the membrane matrix, the solution diffusion model first proposed by Thomas Graham in 1866, can be used to describe the transport mechanism (Figure1.d). According to this model, three steps are involved in gas permeation. The permeant is first sorbed onto the polymer. The permeant then diffuses through the polymer structure, to be ultimately desorbed at the opposite polymer surface

(DeNaylor, 1989). Solution diffusion model has the most direct commercial relevance having simultaneously high selectivity and permeability.

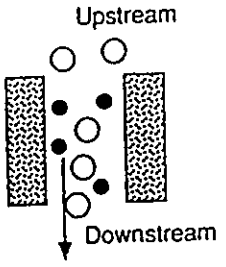

1 a. Viscous flow

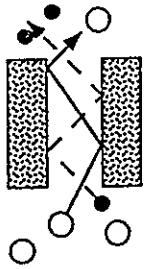

1 b. Knudsen flow

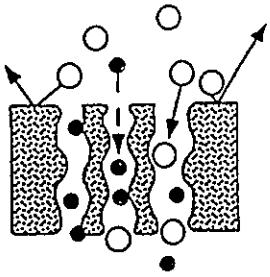

1 c. Molecular sieving

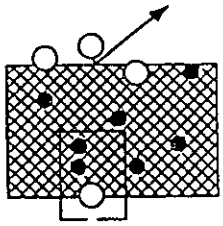

1 d. Solution diffusion

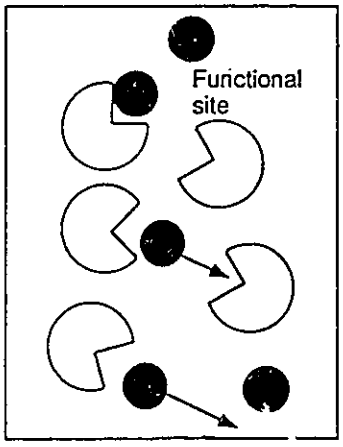

1 e. Activated transport

Figure 1: Transport mechanisms

1.6 Models for Gas Transport

In order to explain permeant diffusion through polymer matrix, a number of theories have been postulated. Models describing gas transport through homogeneous membranes generally depend on whether the polymer in its "rubbery" or "glassy" state.

1.6.1 Matrix Model

A model describing gas sorption and transport in glassy polymers has been proposed by Raucher and Sefick (1983 a& b). The so called matrix model is based on the assumption that gas molecules exist in a glassy material as a single population. The peculiar form of the sorption and permeability concentration dependence is due to gas polymer interaction which was assumed to be strong enough to change the polymer's structure properties by altering the interchain potential energy.

1.6.2 Dual-Mode Model

The Dual-Mode sorption model describes gas solubility in glassy polymers. Inherent in the dual-mode sorption model is the concept of sorption into two idealized environments (Barrer et al., 1958; Micheals, et al., 1963). One population of sorption is viewed as arising from uptake into a dissolved environment similar to sorption in low molecular weight liquids and rubbery polymers, and is described by Henry's law. The second population of sorption is viewed as being due to uptake into the unrelaxed volume or "microvoids" present in glassy polymers. This population of sorption is described as the Langmuir "hole filling" process.

1.6.3 Free-volume Diffusion Model

The free-volume theory of diffusion in polymers was first developed by Fujita et al. (1960) and Fujita (1961& 1968) and since its development several versions have evolved (Frisch et al., 1971; Stern et al., 1983). The premise for free-volume diffusion in polymers is the free volume theory of diffusion, developed primarily through the works of Duda, Vrentas and Frisch et al. (1976, 1977 b) and Frisch et al. (1971). Although simple and useful versions of the theory have been developed, the primary challenge in applying the theory is providing precise physical definitions for free volume parameters.

The free volume theory of transport postulates that movement of molecules depends on the free volume available as well as the availability of energy sufficient to overcome polymer-polymer attractive forces (Vrentas and Duda, 1986). They propose that the specific volume of the polymer and polymer-penetrant mixture is comprised of three components:

(1) The occupied volume, which is the volume of the equilibrium liquid at 0°K.

(2) The interstitial free volume, which is small and distributed uniformly through material transport.

1.7 Literature Survey

1.7.1 Effect of Reactor Design:

The effect of reactor design for plasma polymerization has raised considerable interest among researchers in recent years. A study was carried out using different flow patterns in a tube-type reactor as shown in Figure 2 (Yasuda and Hirotsu, 1978).

Yasuda and his co-workers have conducted extensive experiments to determine the conditions of systems for optimum deposition and deposition location. As an example, different flow patterns with respect to the position of the plasma-forming region (coil) are shown in Figure 3. In design I, a monomer is fed through a tube in the direction of flow into the center of the reaction vessel, while in design II it is directed against the flow. In design III, the flow is reversed, in IV the monomer is directed through the coil into the end of the reactor, and in design V this flow is reversed. In this reactor design, the diameter of the tube portion that is surrounded by the R.F. coil was made smaller than that of the main part of the reaction tube. In this manner, the amount of polymer deposition under the coil was reduced so that a large tail-flame portion of glow discharge could accommodate plasma deposition. The intent was to decouple the initial impact of electron bombardment and thus reduce many secondary effects that may have overshadowed other elements of the study. The distribution of polymer deposition is expressed by the distance from an arbitrary zero point to the right of the center of the reactor. Foil sheets having dimensions of 1 x 2 cm at 4 cm were placed at 4 cm intervals on a 2.5 x 38 cm glass plate. Their weight increases were determined as a measurement of the deposition rate. The results of these experiments showed no significant differences between the deposition patterns in design I and II, (where the ethylene was injected into

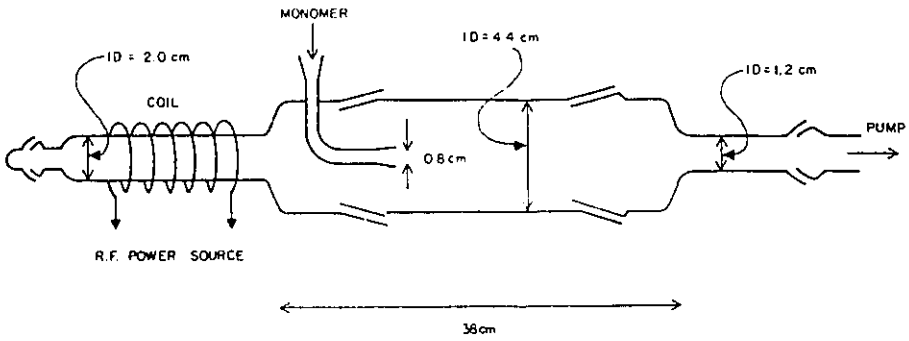

Figure 2: Schematic representation of a standard reactor

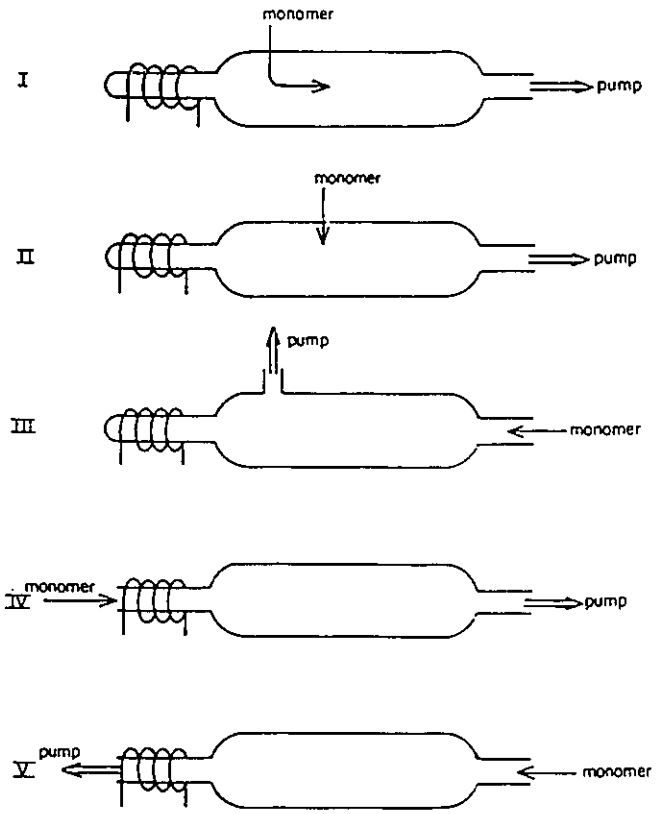

Figure 3: Schematic representation of different flow patterns

the direction of the flow) and the pattern in design II (where injection was perpendicular to the flow).

When the direction of the flow was reversed (designs III and V), a change in the distribution pattern was observed. When the directional flow is reversed (design V), the glow does not extend through the entire length of the reaction tube, therefore no polymer deposition occurs beyond + 8 cm. However the glow was observed to penetrate into the outlet tube in design III. No marked differences in polymer deposition patterns were observed when comparing designs III and V. When the reactor is located downstream of the R.F. Coil, the glow is found to extend through the entire length of the tube. With AC discharges on the electrodes, the best results were obtained at higher frequencies. At higher discharge frequencies, more energy is transferred to the gas where angular frequency, ν between electrons and the gas, at a pressure of 1 hour, $\nu=10^{9}sec^{-1}$ corresponds to a discharge frequency of about 160 MHz. In a bell jar reactor, a large volume of monomer surrounds the plasma zone and monomer flow is less effective, so that diffusional transport dominates. Film deposition occurs on the electrode, on the material placed on the electrode or between electrodes. A different deposition pattern is observed depending on the arrangement of polymer collection. It is found that the deposition rate is highest at the center of the electrode. The deposition patterns, explored by (Yasuda, 1984) using the following designs for monomer feed in a bell jar reactor (Figure 15), are shown in Figure 16. The minor asymmetry of the polymer deposition pattern is attributed to the flow pattern over the entire reactor system. It can be seen that the principle governing the tube type reactor remains essentially the same as the bell-jar type reactor. Due to the predominance of diffusional types of transport, the polymer deposition of the plasma species is non-uniform.

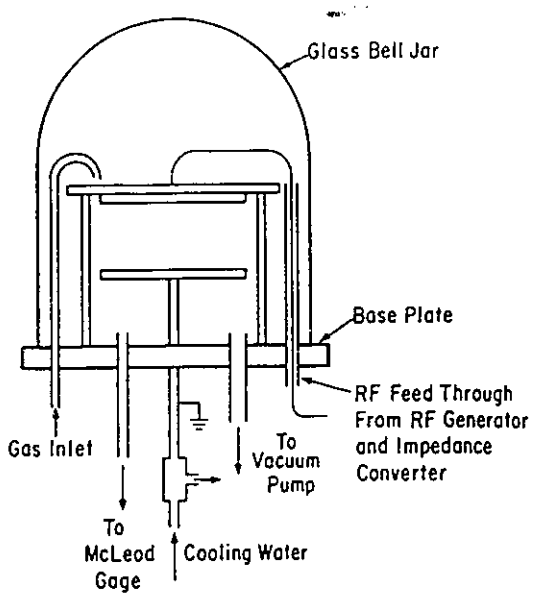

Figure 4: Schematic diagram of the bell-jar reactor

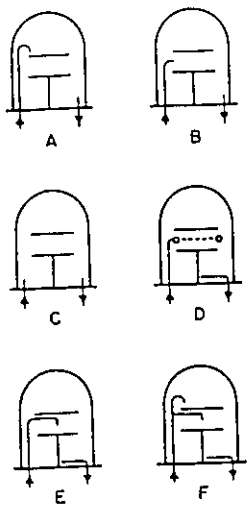

Figure 5: Schematic diagram of the inlet-outlet configuration of the bell jar reactor

As the pressure of the system is decreased the variations become smaller, since the diffusional displacement distance of the plasma particles increases with lower pressure.

On wall surfaces further away from the electrodes, polymer deposition is smaller than on the electrode surfaces due to less intense plasma (glow) in the region away from the electrodes. Deposition thickness is generally found to decrease with increasing distance from the electrode center.

1.7.2 Methods of Plasma Polymer Characterization:

Plasma polymers are generally insoluble, amorphous thin films and therefore not amenable to many of the characterization techniques appropriate for conventional polymers. Applicable techniques include surface analytical probes (ESCA or XPS, contact angle, ATR FTIR), techniques which determine component parts of the plasma polymer (pyrolysis/GC or MS, elemental analysis, or solid state NMR), or those yielding information regarding chemical species in the plasma from which deductions can be made regarding the plasma polymer product (e.g., residual gas analysis, optical emission analysis, laser induced fluorescence). The morphology of plasma polymers can be determined by electron microscopy (scanning and transmission) and by small angle X-ray scattering. Electron spin resonance has been used to identify the population of stable free radicals in given plasma polymers. Examples of these techniques are provided.

1.7.2.1 Surface Analytical Techniques:

1.7.2.1.1 X-Ray Photoelectron Technique

X-ray photoelectron spectroscopy (XPS), also known as electron spectroscopy for chemical analysis (ESCA), is a surface analysis technique which gives qualitative and semi-quantitative(± 10 %) information for all elements except hydrogen and helium. The technique has its basis in the photoelectric effect. The sample is exposed to monoenergetic x-ray; interaction of the x-rays with atoms in the sample results in photoemission of electrons (see Figure 6) which are subsequently sorted based on their kinetic energy (KE). The KE of the photoelectron is a function of the atomic and molecular environment of origin. The data obtained are plotted as intensity (i.e. the number of electrons detected, or counts) versus KE or, more commonly, the binding energy (BE) of the electrons.

The fundamental equation of XPS which relates these terms is

$$KE = h\nu - BE - \emptyset s$$

where KE = kinetic energy of emitted electrons

BE = binding energy of emitted electrons,

$h\nu$ = energy of x-ray photon,

and $\emptyset_S$ =work function of spectrometer (characteristic of each individual instrument - a constant)

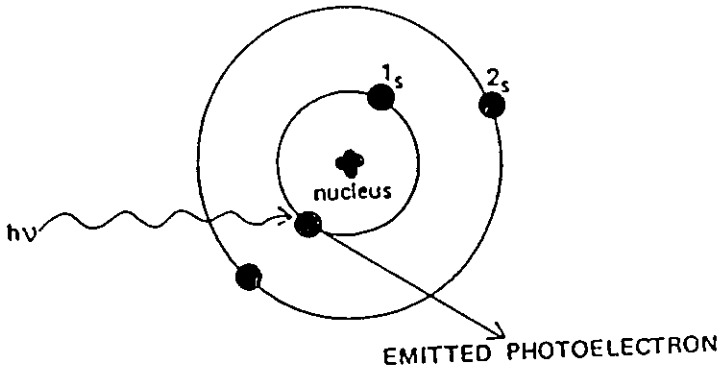

Figure 6: A Schematic view of the interaction of an X-ray photon of energy hν with an atomic orbital electron (Andrade, 1985)

The plot of intensity vs. BE results in a spectrum in which each element causes unique peaks. The area under each peak is normalized according to the sensitivity. Further information about chemical state can be obtained from exact peak locations and separations. Of particular interest is C_{1s} region.

The photons of the x-ray penetrate into the sample to a depth in the order of several microns. However, due to the low mean free path of photoelectrons (tens of Angstroms), only those electrons emitted from atoms in the top 10-20 atomic layers emerge to be continued with no KE loss. It is these electrons which contribute to the main spectral peaks. Other electrons escape the specimen after undergoing energy loss processes and contribute to the back ground of the spectrum. Figure 7 illustrates these two events.

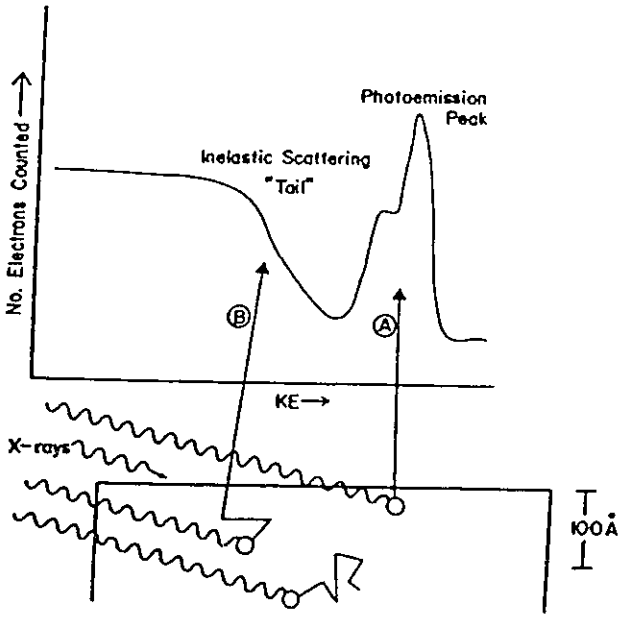

Figure 7: X-ray induced photoemission of electrons from an atom near the surface and from atoms further into the bulk. Surface electrons which escape without undergoing energy loss process (A) contribute to the photoemission peak. For atoms somewhat deeper into the specimen, interaction of emitted electrons (B) with other atoms has a greater probability of occurring. The loss of kinetic energy from such an interaction results in the appearance of an inelastic scattering tail in the spectrum (Ratner, 1986)

Insulating samples present the additional problem of net positive charge accumulation at the surface due to photoelectron emission. This creates an electric potential which must be overcome by the emitted electrons, decreasing their KE, and thus increasing the calculating BE. This is usually remedied by the use of an electron flood gun. Thermionically emitted electrons of low energy are directed at the surface where they neutralize positive charges.

Non destructive depth profiling can be achieved by varying the angle of the sample surface with respect to the electron analyzer system. As demonstrated in Figure 8, the effective sampling depth is reduced proportionately to cos θ.

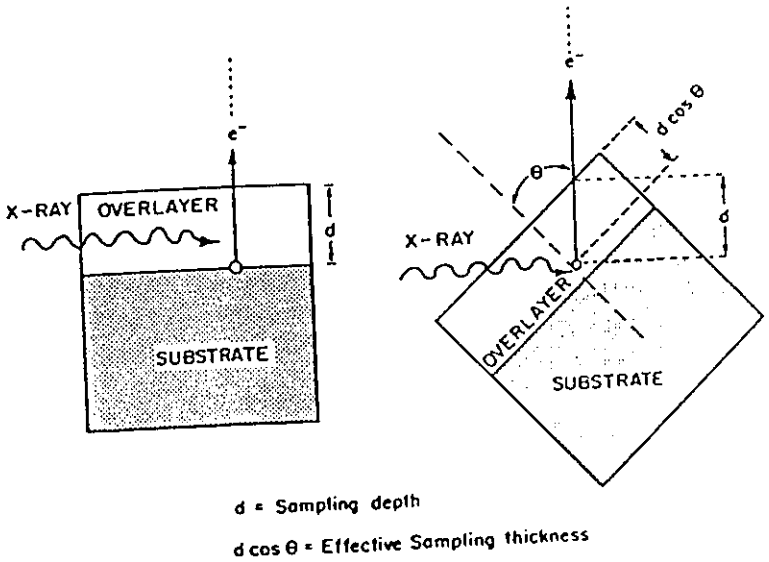

Figure 8: Decrease in the effective sampling depth as the angle of the specimen is increased with respect to the horizontal (Ratner, 1986)

1.7.3 Contact Angle:

Contact angle has been defined as the angle between the solid surface and the tangent of the liquid-vapor interface of a sessible drop (Zisman, 1964) for a water droplet on a polymer surface. The contact angle approaches zero (the drop spreads out over the surface) for a hydrophillic surface and increases for increasingly hydrophobic surfaces. The measurement of contact angles of various liquids (a minimum of 2) on a solid smooth yields the free energy of the surface γ_{sv} and its dispersive and polar components (γ^{d}_{sv} and γ^{p}_{sv} respectively). While not identifying the functional groups at the surface, these quantities are obviously sensitive to the chemical nature of the surface,
and are affected by its roughness and the presence of holes and pores. When compared with ESCA, the technique has been demonstrated to be more sensitive to the immediate surface (Anand and Baddour, 1981).

1.7.4 Pyrolysis/GC and Pyrolysis/MS:

Pyrolysis/GC and pyrolysis/MS have been used to obtain information regarding plasma polymer microstructure. An example of this method to the analysis of hydrocarbon plasma polymers is found in the study of the plasma polymerization of ethylene (Seeger et al., 1975) and of acetylene, butene, benzene and butadiene (Seeger et al., 1977).

1.7.5 Solid State NMR:

Solid state NMR has been used in a limited number of cases to identify the microstructure of plasma polymers. This powerful technique is at present of limited applicability

because of the relatively large sample mass required (20 mg for ^{13}C NMR in natural abundance). The microstructure of plasma polymers obtained using the monomers ethane, ethylene, acetylene, toluene, tetrafluorethylene, and fluorotoluene were studied using ^{13}C NMR by Dilks and co-workers (Kaplan and Dilks, 1984; Kaplan and Dilks, 1981; Dilks and Kaplan , 1982).

1.7.6 Elemental Analysis:

Elemental analysis is an important characterization technique for plasma polymers. Because quantitative data is readily available, the method can be related to cross-link density and to the degree of organic structure (siloxane plasma polymers). It is especially important for determination of hydrogen content, which cannot be directly obtained from ESCA.

1.7.7 Infrared Spectroscopy:

Infrared spectroscopy is used for functional group identification. It has been used to quantitatively gauge the concentrations of functional groups in plasma polymers and hence the crosslink density of hydrocarbon plasma polymers (Tibbitt et al., 1976; Kobayashi et al., 1974; Tibbitt et al., 1977).

Infrared spectroscopy can also be used to increase the versatility of ESCA and to qualitatively show the presence of functional groups by providing a semiquantitative measure of their concentration (Morosoff et al., 1984; Morosoff et al., 1985). IR spectra can be obtained by depositing the plasma polymer on infrared transparent substrates or on other surfaces by using techniques such as ATR (attenuated total reflectance).

1.7.8 Electron Spin Resonance:

ESR is an important characterization technique for plasma polymers (Scott et al., 1979; Song et al., 1983; Nakamura, et al., 1981) because of their customary cargo of relatively air-stable free radicals. ESR spectra have been obtained for plasma polymers, as deposited (i.e, in vacuum) (Nakamura et al, 1981), after exposure to air and after various thermal and environmental post treatments (Morinaka and Asano, 1982; Grenda and Venugopalan, 1980; Morita et al., 1971).

1.7.9 Morphological Analysis

1.7.9.1 Electron Microscopy

The techniques most widely used to obtain information regarding the morphology of plasma polymer thin films and powders are transmission electron microscopy (TEM) and scanning electron microscopy (SEM). These tools have been used to determine the size of powder particles (Liepins and Sakaoku, 1972) or to demonstrate the presence of powder particles in thin films (Tkachuk and Shustov, 1975; Thompson and Smolinsky, 1972; Biederman, 1981; Biederman et al., 1977; Havens et al., 1978).

1.7.9.2 Small Angle X-Ray Scattering:

Small angle x-ray scattering (SAXS) in an excellent technique for the detection of density inhomogeneities in condensed matter. It is complementary to electron microscopy because the smaller the dimension of the inhomogeneity, the easier it is detected by

SAXS in the range of 15-4000 Å. SAXS has been used to detect globular inhomogeneities in ethylene and styrene plasma polymers (in the range 0.2 - 0.4 microns, 70 % by volume of spheres) (Havens, et al., 1978).

Chapter 2

Theory

2.1 Resistance Model

Composite membranes are being used in various membrane separation processes including gas separation, reverse osmosis and pervaporation. There has been a lack of success in the development of a thin film composite membrane for gas separation. This failure is due principally to the difficulty in developing a straightforward process for producing large quantities of highly permselective membranes with permeation rates sufficiently high to be economically viable.

In the past, composite membranes were made by supporting a thin separating membrane on a porous substrate to achieve high fluxes. In these membranes the coating serves as the separating barrier, and the substrate serves only as a physical support function .

In the 80's Henis and Tripodi (1980 a& b) developed a resistance model to explain the behavior of composite gas separation membranes which consist of a porous asymmetric substrate of one polymer, and a coating of a second polymer. According to

the resistance model, the membrane is divided into different segments and each segment provides different resistance to the permeating gas. These resistances are analogous to the resistance to the flow of electricity in an electric circuit. In the following sections the resistance of each membrane segment is represented by its electrical analog.

The permeation rate (flux) for the gas component i through a polymeric membrane can be described by:

$$Q_i = \frac{P_i A \Delta p_i}{l} \tag{1}$$

where Q_i is the permeation rate of component i, P_i is the permeability of the polymer material to component i, A is the cross sectional surface area of the membrane available for permeation , l is the thickness of the membranes through which the component permeates, and Δp_i is the partial pressure difference of component i across the membrane.

Using the electrical analog, the above relationship describing permeation through a polymer membrane is mathematically equivalent to Ohm's law which describes the current flow through a resistor:

$$I = \frac{E}{R} \tag{2}$$

Conceptually the current, I, can be equated with the permeation rate, Q_i. The driving force for current flow, (i.e. the difference in electric potential E), is analogus to the pressure difference across membrane Δp_i. We can define then, a resistance to permeate flow, R_i which is equivalent to the electrical resistance R_i.

$$R_i = \frac{l}{P_i A} \tag{3}$$

By combining equation (1) and (3)

$$Q_i = \frac{\Delta p_i}{R_i} \tag{4}$$

Figure 9 shows a schematic representation of an uncoated asymmetric membrane used as a substrate for coating or lamination and it's electrical analog.

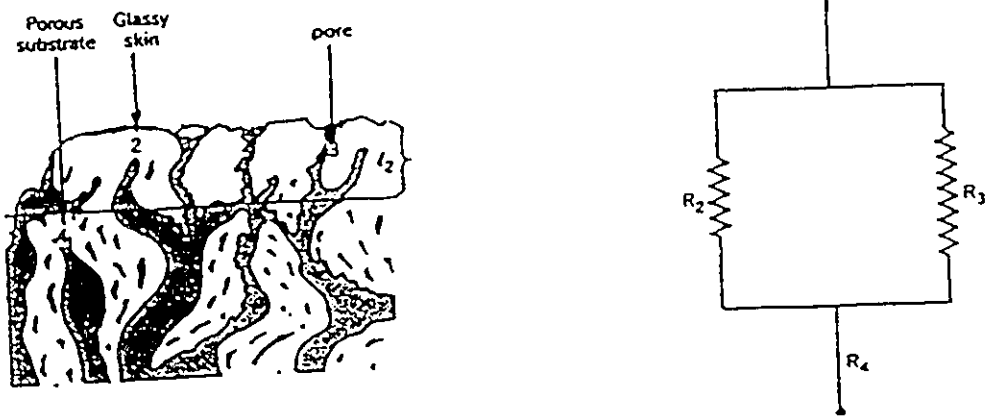

Figure 9: Asymmetric membrane and electric circuit analog

We define three regions in this substrate membrane: the surface region or skin, of thickness l_2, denoted as 2 in the Figure; the defects or pores in this skin, denoted as 3; and the highly porous matrix region, denoted as 4.

The total resistance to permeate flow, $(R_t)_i$, in the porous substrate membrane is a function of the resistance of dense portions of the surface region, R_2, the resistance of the pores in the surface, R_3, and the resistance of the porous matrix R_4. The functional relationship between R_2, R_3 and R_4 which describes the total resistance, analogous to the relationship between resistances in an electrical circuit, is expressed as follows:

$$(R_t)_i = \frac{1}{\frac{1}{(R_2)_i}+\frac{1}{(R_3)_i}} + (R_4)_i = \frac{(R_2)_i(R_3)_i}{(R_2)_i+(R_3)_i} + (R_4)_i \qquad (5)$$

Figure 10 shows a schematic representation of the cross sectional area of a composite membrane prepared by applying a defect free coating material to the substrate membrane illustrated in Figure 9, along with its electrical circuit analog. The permeation behavior is related to the resistance to gas flow of four elements: the dense portion, $(R_2)_i$, the pores in the skin layer, $(R_3)_i$, the open internal structure, $(R_4)_i$, and the coating material, $(R_1)_i$. By using Ohm's law for resistors in parallel and series, the total resistance of permeation through a laminated composite membrane $(R^L)_i$ can be derived:

$$(R^L)_i = (R_1)_i + \frac{(R_2)_i(R_3)_i}{(R_2)_i+(R_3)_i} + (R_4)_i \qquad (6)$$

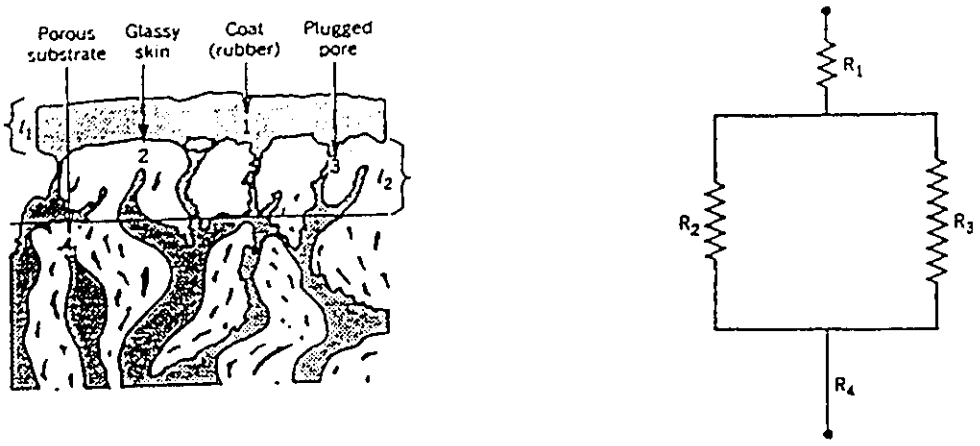

Figure 10: Coated membrane and electric circuit analog

According to Henis and Tripodi a membrane with high flux and good separating properties will have very open internal structures, and $(R_4)_i$ should be very small relative to $(R_1)_i$, $(R_2)_i$ and $(R_3)_i$. In such cases, equations (5) and (6) simplify to:

$$(R_t)_i = \frac{(R_2)_i (R_3)_i}{(R_2)_i + (R_3)_i} \tag{7}$$

$$(R^L)_i = (R_1)_i + \frac{(R_2)_i (R_3)_i}{(R_2)_i + (R_3)_i} \tag{8}$$

Although the Resistance Model explains the behavior of composite gas separation membranes which consist of a porous asymmetric substrate of one polymer

and a coating of a second polymer , it fails to describe membranes with a layer laminated with a second polymeric membrane since the plugging of pore is assumed.

2.2 Modified Resistance Model

2.2.1 Development of Modified Resistance Model

A modified resistance model has been established by Matsuura et al., (1989). The new model is a special case of the Wheatstone Bridge of the electrical circuit. The resistance model proposed by Henis and Tripodi is considered as a special case of the new model and can be used when the substrate membrane is either coated or laminated with a second polymer on the top.

As before the total resistance of the porous asymmetric membrane to the permeate flow, $(R_t)_i$, is composed mainly of two elements: $(R_2)_i$ the resistance of gas flow through the polymer matrix of the membrane and $(R_3)_i$ the resistance of gas flow through the pores on the surface of the membrane. The resistance of the open porous structure beneath the skin layer is assumed to be negligible compared to the other two resistances. Figure 11 shows the membrane and the electrical analog. By using Ohm's law for resistors in parallel the total resistance to permeate flow, $(R_t)_i$ can be divided as follows:

$$\frac{1}{(R_t)_i} = \frac{1}{(R_2)_i} + \frac{1}{(R_3)_i} \tag{9}$$

$$\frac{1}{(R_t)_i} = \frac{(R_2)_i + (R_3)_i}{(R_2)_i (R_3)_i} \tag{10}$$

$$(R_t)_i = \frac{(R_2)_i (R_3)_i}{(R_2)_i + (R_3)_i} \tag{11}$$

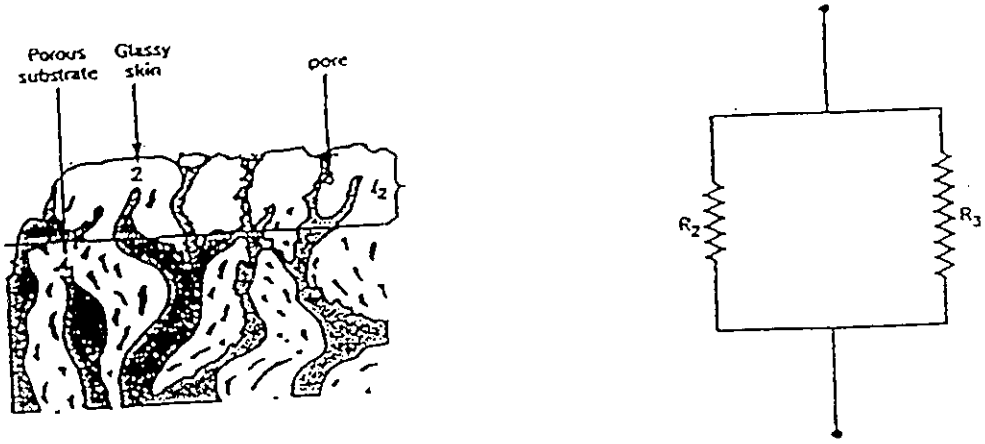

Figure 11: Asymmetric membrane and electric analog

The new resistance model is a special case of the Wheatstone Bridge model and is schematically illustrated in Figure 12. The Figure shows all the component resistances involved in a composite membrane that consists of a silicone membrane laminated on the

top of a porous polymeric sublayer with its electrical analog. Referring to the porous sublayer, gas can permeate through the membrane by entering the polymer matrix and passing through it with a resistance $(R_2)_i$, whereas $(R_3)_i$ is the resistance to the gas flow through the pore. Referring to the laminated silicone membrane, $(R_1)_i$ is the resistance for the flow of the gas through the silicone layer that covers the area occupied by the polymer matrix of the porous sublayer, whereas $(R_{1'})_i$ is the resistance for the gas flow through the silicone layer that covers the area occupied by the pores. The overall resistance of the laminated membrane is given by:

$$(R^L)_i = \frac{[(R_1)_i + (R_2)_i][(R_{1'})_i + (R_3)_i]}{[(R_1)_i + (R_2)_i + (R_{1'})_i + (R_3)_i]} \tag{12}$$

There may also be a cross flow resistance connecting $(R_1)_i + (R_2)_i$ and $(R_{1'})_i + (R_3)_i$. The resistance for this flow is called $(R_x)_i$. This cross flow resistance is infinity when the gas flows only in the vertical direction. By using Ohm's law for resistors in series and parallel we can obtain the overall resistance of a porous membrane with lamination.

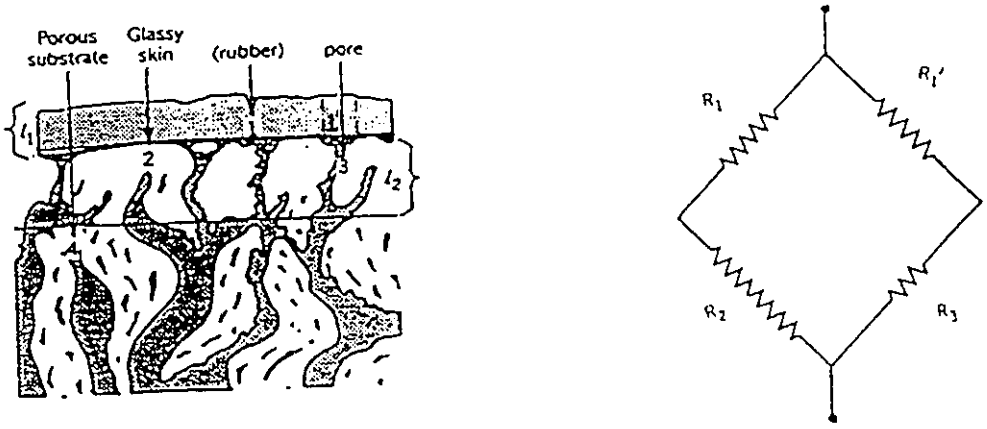

Figure 12: Laminated membrane and electric analog

2.2.2 Method to Determine Local Resistances

An example is given in the following to solve the local resistances for O_2 and N_2 gases from the overall resistance $(R_t)_i$ (i=O_2 or N_2) for the porous substrate membrane and $(R^L)_i$ (i = O_2 or N_2) for the laminated membrane. Both $(R_t)_i$ and $(R^L)_i$ are obtained from equation 4 using permeation rate data Q_i, of the porous substrate and the laminated membrane.

The ratio of the resistances of the flow of N_2 to that of O_2 is given as follows: Based on the overall resistance of the substrate membrane

$$\alpha_t = \frac{(R_t)_{N_2}}{(R_t)_{O_2}} = \frac{(Q_t)_{O_2}}{(Q_t)_{N_2}} \tag{13}$$

Based on the overall resistance of the laminated membrane

$$\alpha^L = \frac{(R^L)_{N_2}}{(R^L)_{O_2}} = \frac{(Q^L)_{O_2}}{(Q^L)_{N_2}} \tag{14}$$

Based on the individual regions

$$\alpha_j = \frac{(R_j)_{N_2}}{(R_j)_{O_2}} \tag{15}$$

Where j = 1, 2 and 3

$$\alpha_j = \frac{(P_j)_{O_2}}{(P_j)_{N_2}} \tag{16}$$

and $\alpha_{1'} = \alpha_1$

The last equation is valid since both α_1 and $\alpha_{1'}$ are the ratios corresponding to silicone rubber material. Using the ratios defined above, the overall resistances of a substrate for O_2 and N_2 are written by equation 11 as:

$$(R_t)_{O_2} = \frac{(R_2)_{O_2}(R_3)_{O_2}}{(R_2)_{O_2} + (R_3)_{O_2}} \tag{17}$$

$$\alpha_t(R_t)_{O_2} = \frac{\alpha_2(R_2)_{O_2}\alpha_3(R_3)_{O_2}}{\alpha_2(R_2)_{O_2} + \alpha_3(R_3)_{O_2}} \tag{18}$$

The overall resistance of a laminated membrane, on the other hand, can be written as:

$$(R^L)_{O_2} = \frac{[(R_1)_{O_2} + (R_2)_{O_2}][(R_{1'})_{O_2} + (R_3)_{O_2}]}{[(R_1)_{O_2} + (R_2)_{O_2} + (R_{1'})_{O_2} + (R_3)_{O_2}]} \tag{19}$$

and

$$\alpha^L(R^L)_{O_2} = \frac{[\alpha_1(R_1)_{O_2} + \alpha_2(R_2)_{O_2}][\alpha_1(R_{1'})_{O_2} + \alpha_3(R_3)_{O_2}]}{[\alpha_1(R_1)_{O_2} + \alpha_2(R_2)_{O_2} + \alpha_1(R_{1'})_{O_2} + \alpha_3(R_3)_{O_2}]} \tag{20}$$

The last equations are from equation 12 of the modified resistance model. Because the substrate membrane remains unfilled when it is laminated with silicone membrane, these last equations can be used.

An assumption is made to reduce the number of variables from equations 17 to 20; i.e. the area of the polymer matrix, A_1, is approximated by that of the total area, $A_t = A_1 + A_{1'}$. This can be justified since $A_1 >> A_{1'}$, since the pore area is much smaller than the membrane area. Then applying equation 3

$$(R_1)_i = \frac{l_1}{(P_1)_i A_1}$$

for the i gas component (i = O_2 or N_2). Since the thickness of the silicone rubber , l_1, the intrinsic permeability of silicone rubber, $(P_1)_i$ (see Table 2), and the total area are known $(R_1)_i$ can be calculated for (i = O_2 and N_2). Therefore, $(R_1)_{O_2}$ and $\alpha_1 (= \frac{(R_1)_{N_2}}{(R_1)_{O_2}})$ are known quantities.

Furthermore, intrinsic permeability data, P_2's, will be given for O_2 and N_2 later in the discussion section. Using those values $\alpha_2 (= \frac{(P_2)_{O_2}}{(P_2)_{N_2}})$ can be calculated.

Now looking into equations 17 to 20, there are four unknowns $(R_{1'})_{O_2}$, $(R_2)_{O_2}$, $(R_3)_{O_2}$ and α_3. Therefore, these unknowns can be obtained numerically by solving equations 17 to 20 by the following steps:

Step 1 Solve equations 19 and 20 for $(R_{1'})_{O_2}$ and $(R_2)_{O_2}$ assuming $(R_3)_{O_2}$ approaches zero.

Step 2 Solve equations 17 and 18 for α_3 and $(R_3)_{O_2}$ with the value of $(R_2)_{O_2}$ obtained in Step 1.

Step 3 Once again, solve equations 19 and 20 using the revised $(R_3)_{O_2}$ and α_3 values.

Step 4 Again solve equations 17 and 18 for α_3 and $(R_3)_{O_2}$ with the value of $(R_2)_{O_2}$ calculated in step 3.

Step 5 Repeat steps 3 and 4 until the value of $(R_3)_{O_2}$ value for both steps are the same.

The same principle can be applied to obtain local resistances for CO_2 and CH_4 with corresponding intrinsic permeability data, (see Table 2) in silicone rubber and those for polyethersulfone.

Chapter 3

Experimental

3.1 Material

The polyethersulfone membranes used were those made by the National Research Council from PES Victrex 200 P and of molecular weight cut off 5000.

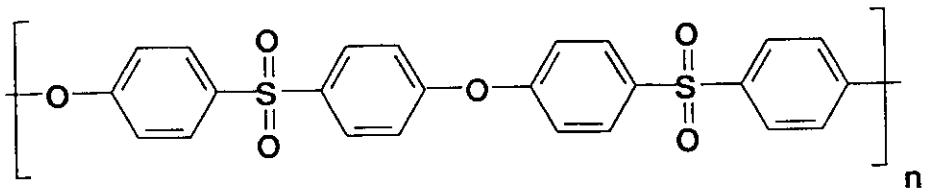

POLYETHERSULFONE PES VICTREX

For preparation of dry membranes, the water in the membranes is replaced by a water miscible first solvent. The first solvent is then replaced by a second solvent which is volatile and allowed for simple air drying of the membrane (Minhas et al., 1985). In this project iso-propyl alcohol was used as the first solvent and hexane second. Four iso-propyl alcohol/water solutions were prepared containing 25%, 50%, 75%, and

100% (v/v) iso-propyl alcohol/water. The membrane coupons were kept in stirred solutions of each of the alcohol/water solutions for 24 hours starting with 25%. Finally the coupons were transferred to a 100% hexane bath and kept for another 24 hours, and then they were dried. The whole procedure was performed at room temperature. Some of the PES membranes were laminated with a 38 μm layer of polydimethylsiloxane (silicone rubber) supplied by Mempro (Membrane Products Company). The intrinsic permeabilities of various gases through this silicone membrane (as observed by the manufacturer, Mempro) are shown in Table 2. The silicone rubber membrane has a homogeneous morphology.

Table 2: Intrinsic permeabilities of various gases through polydimethylsiloxane membrane.

Gas	CO_2	CH_4	H_2	O_2	He	N_2
mol.m/m^2 .s.Pa	9.04E-13	2.68E-13	1.84E-13	1.67E-13	1.00E-13	8.37E-14

Some of the PES membranes were plasma coated with pure aniline using the NRC Plasma Polymerization System shown in Figure 13. Some of the plasma coated membranes were also laminated with 38 μm thickness of polydimethylsiloxane rubber.

3.2 Apparatus

A schematic diagram of the apparatus used for plasma polymerization is shown in Figure 13. An expanded drawing of the chamber from different views is shown in Figure 14. An extensive literature survey was conducted on reactor geometries and summarized in Chapter 1.

The plasma polymerization was carried out in a stainless steel cylindrical chamber (installed in a horizontal position) 134 cm long and 46.5 cm in diameter, with an internal stainless steel tubular type electrode (50 cm long x 4.5 cm in diameter). When looking at a vertical cross sectional view the electrode is located 13 cm above the chamber center and 4 cm to the left of the center.

Gases (monomer and argon as a carrier gas) were carried in a stainless steel tube 0.63 cm in diameter, entering from one end of the chamber, then dividing into two equally sized tubes at the same distance from the electrode (10 cm). In preliminary tests, polyaniline plasma was deposited on aluminum foil samples. PES membranes of 9.62 cm diameter were held under the electrode in a flat position by four small pieces of scotch tape on a flat stainless steel sheet located 16 to 56 cm from the end of the chamber. The surface of the membranes was perpendicular to the gas stream to obtain homogeneous deposition (Yasuda, 1984) especially in the central region of the substrate.

Aniline liquid purified by vacuum distillation (Pavia et al., 1982) was reserved in a glass reservoir covered with aluminum foil in order to prevent coloring of the monomer if it was exposed to light

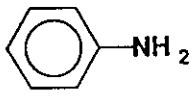

Aniline

One hundred milliliters of purified aniline was injected into the bubbler which was connected to a trap at room temperature and then fed to the chamber. Argon gas was also fed into the bubbler containing the aniline liquid in order to vaporize it. The aniline vapor flow rate of 10 cm^3 (STP)/min. was controlled by a flow meter and a needle valve installed on top of the bubbler.

The vacuum in the system was maintained by a Varian Model SS / SD 700 pump, a Varian Model SD 90 pump, a Varian Model VHS-4-6-250 diffusion pump and measured by an MKS Baratron Model 390 pressure gauge to measure the pressure inside the chamber during plasma polymerization. The gas flow rate was monitored and controlled by a Tylan Model FC-280/ FM-380 Mass Flow Controller/Flow meter. Advanced Energy RFX 13.56 MHz 120 W-2500 W generator was used as power source to produce plasma at the radio frequency of 13.5 MHz.

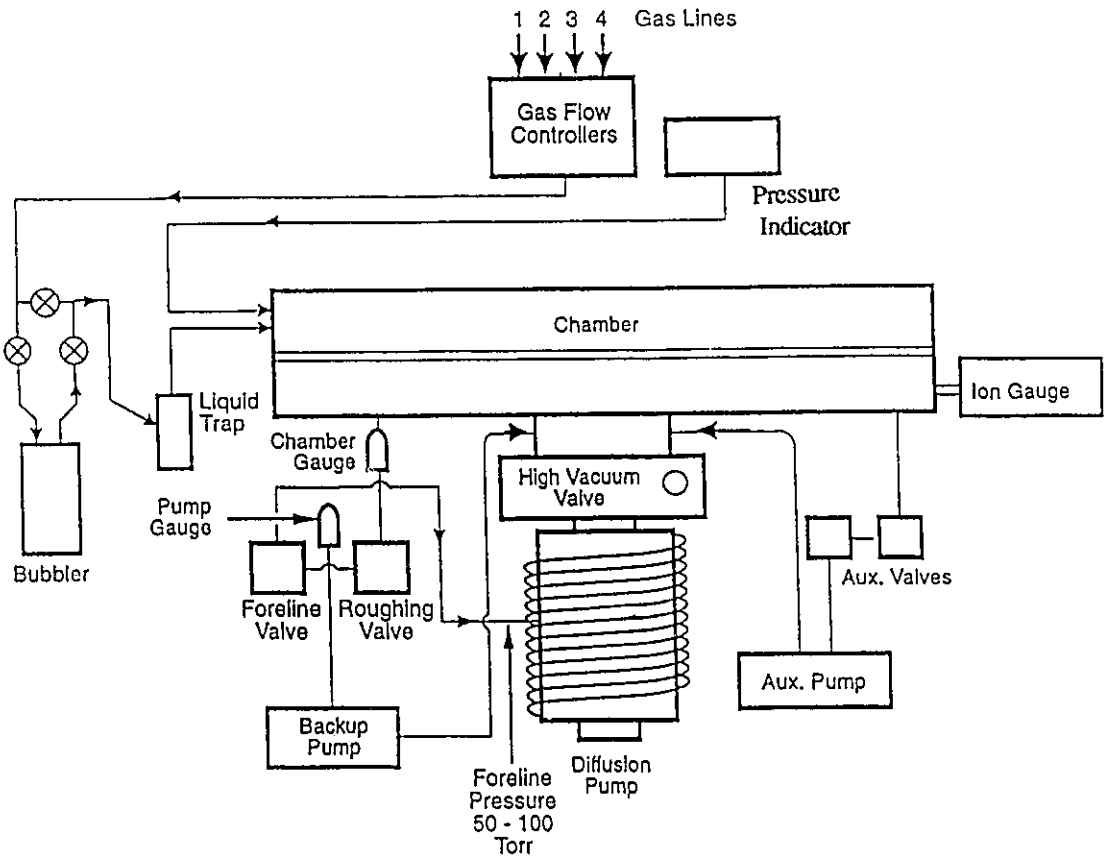

Figure 13: Schematic diagram of the NRC plasma polymerization system

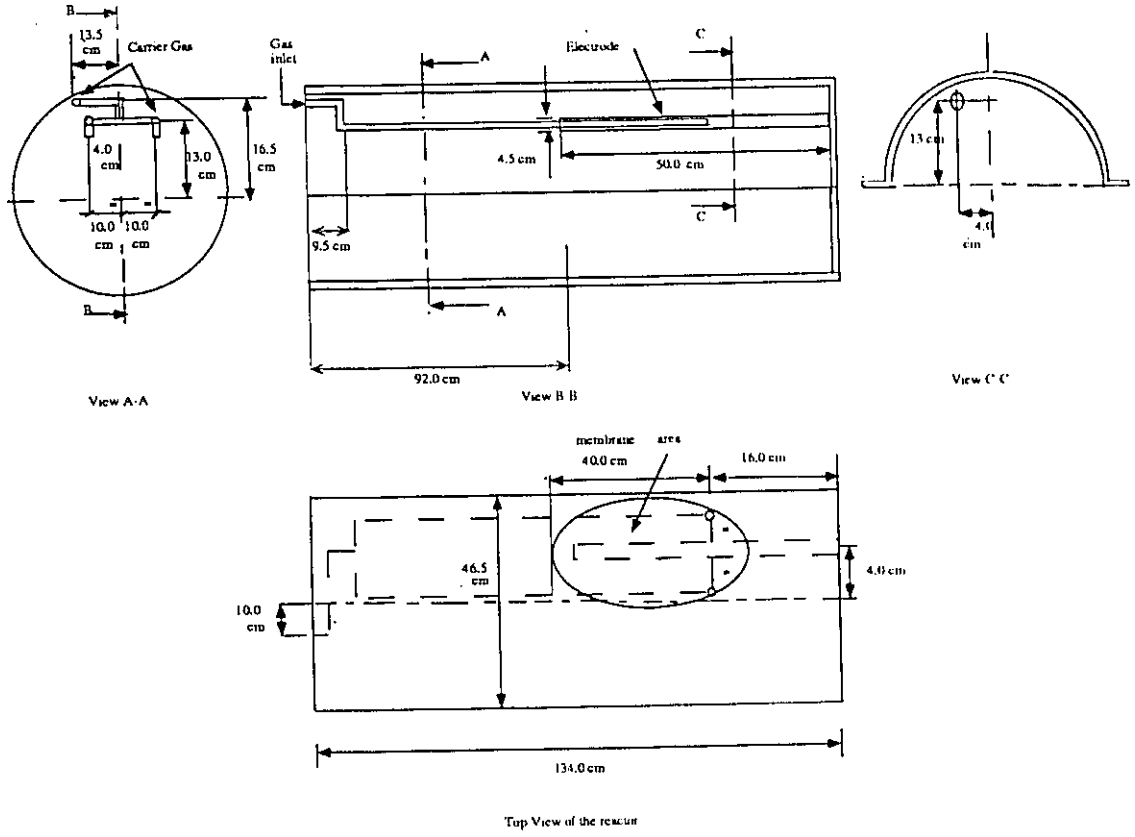

Figure 14: Schematic diagram of the reactor used for plasma polymerization

3.3 Procedure of Plasma Polymerization:

Before starting the plasma polymerization, the chamber was cleaned from inside (the electrode as well as the surfaces that came in contact with the membranes) with ethanol. Before closing the chamber, the diffusion pump was run for 1 hour and the chamber was purged with argon gas in order to get rid of all the air in the feed tubes .

After closing the chamber, it was sealed, evacuated by a roughing pump and then put under high vacuum conditions for approximately 30 minutes until the chamber pressure fell below $5x10^{-5}$ torr. The auxiliary pump was initiated and the baratron was set twice to zero. The gas flow rate was chosen on the mass flow controller and flow commenced. Plasma treatments were performed at a pressure of 0.15 m torr while flow rates were maintained at 10 cm^3 (STP)/min. After the pressure stabilized, the electrode was turned on to generate the radio frequency and set to its chosen value. In this experiment the electrical power supplied to support the radio frequency was 75 W. After a given exposure time (5, 10, 15, 20, 25 min.) the power was shut off at the RFX box. The input gas flow was ceased and the chamber was evacuated using the auxiliary valve to at least 2 m torr. If no further gas treatments were required, the valve between the chamber and the auxiliary pump was closed. Air was then supplied into the chamber and the treated polymer was removed in a covered glass plate to be tested for gas permeation.

3.4 Preparation For Permeation Experiments:

Pure gas permeation experiments were performed with helium, hydrogen, carbon dioxide, oxygen, nitrogen and methane using a cylindrical membrane test cell. A schematic

diagram of the experimental apparatus, along with an expanded drawing of a single permeation cell are shown in Figure 15. Before placing the coupon into the permeation cell both the O-rings and surfaces that came into contact with the membrane were cleaned using ethanol. The membrane skin was left exposed to the gas feed, which entered from the top of the cell. The O-rings were coated with a small amount of silicone grease and put into place. The bottom flange was then fastened to the rest of the cell with six bolts. Helium gas was then passed through the apparatus at 110 psig and all the fittings were checked for leaks using a solution of soap and water. Flow rates were checked to ensure that none of the coupons were damaged. Once no leaks were detected at 110 psig the pressure was increased to 300 psig and the system was checked again for leaks and damaged coupons before beginning the permeation experiments.

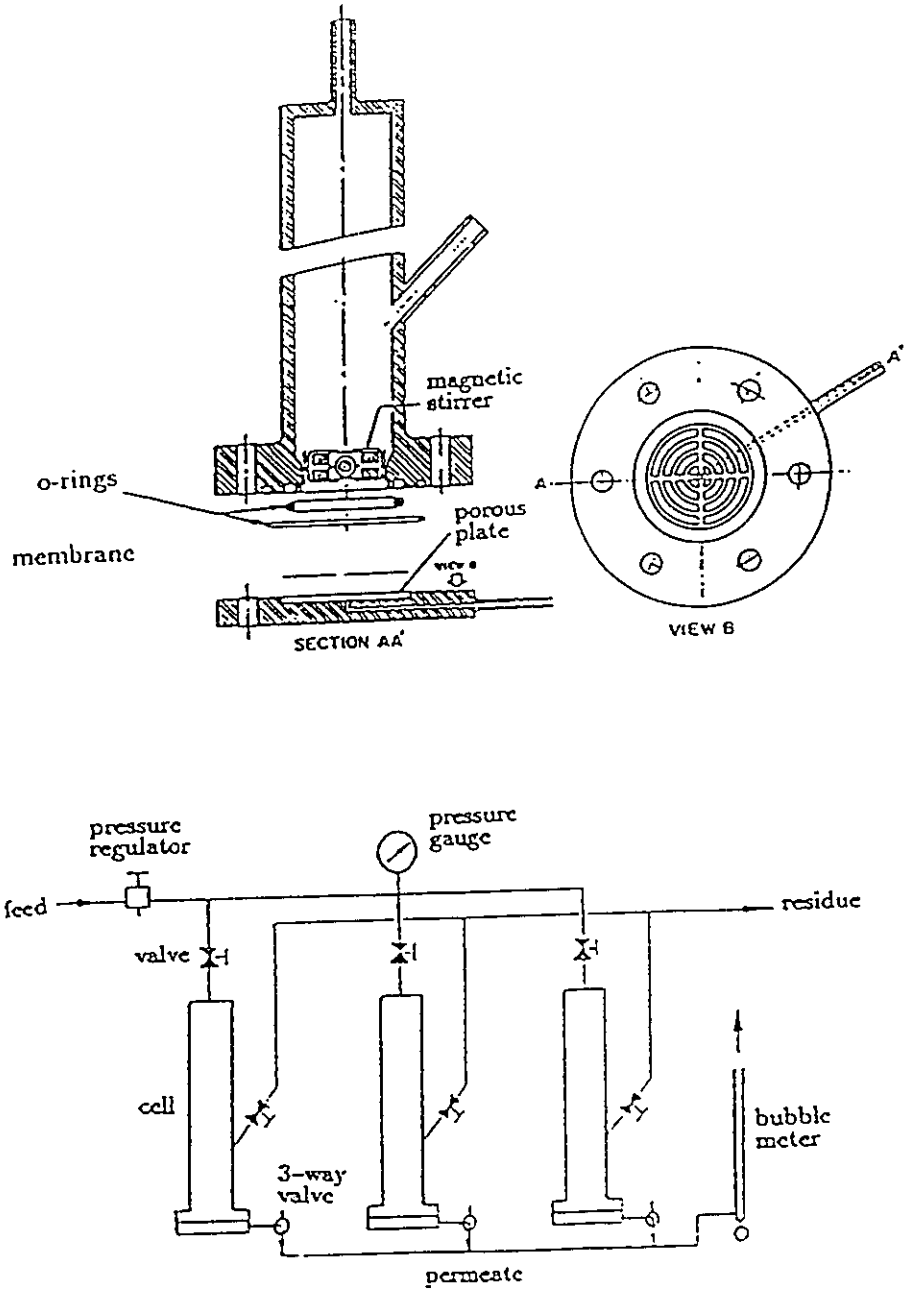

Figure 15: Permeation cell and schematic diagram of experimental apparatus

3.5 Permeation Experiments:

The steady-state permeation rates at different operating pressures (recorded as psig, but converted to kPag) were measured at room temperature and pressure with a bubble flow meter. All gases were supplied by Air Products with a purity of 99.9 %.

The experimental data collected as volume flow rate for different gases at different pressure gradients was first corrected to standard temperature and pressure and then converted to permeability coefficients, A_G (kmol/m^2.s.Pa). The effective area of the membrane used for the permeation studies was 9.62 x 10^{-4} m^2. The coefficient, A_G is the amount of gas permeated per unit time, per unit area, per unit differential pressure across the membrane.

All membranes were tested with gases in the following order: He, H_2, O_2, N_2, CH_4 and then CO_2. Permeation experiments were performed with dry PES, laminated PES, polyaniline plasma coated PES. The gas was supplied from pure gas cylinders and the pressure was kept at 110 psig. Experimental data was collected every 15 minutes until flux data became consistent. After testing each membrane for gas permeation, the entire apparatus was flushed several times with the new gas and the same procedure was repeated.

3.6 Gas Chromatograph Calibration:

Gas chromatography Varian model 3600 was used to measure the gas composition. The position of the peak related to each gas was identified by injecting a pure gas sample into the carrier gas stream and recording the response. According to the studies of Dietz (1967), in order to obtain an accurate composition of the product gas, the gas

chromatography peak area must be divided by a correction factor which is unique for each gas. This correction factor is called the "Thermal response factor" (TRF). Dietz suggested the following TRF's for the gases used in this study; CH_4= 35.7, N_2=42, O_2=40, CO_2=48. The error margin for the above factors is 3 %.

Mohammadi (1994), developed new values of TRF's for methane and carbon dioxide within the error margin reported by Dietz. These values are shown in Table 3.

Table 3: Thermal response factors calculated for carbon dioxide and methane

composition (mol fraction)		TRF	
CO_2	CH_4	CO_2	CH_4
0.25	0.75	50	35.7 ± 0.4
0.50	0.50	50	37.8 ± 0.6
0.75	0.25	50	36.3 ± 0.3
average thermal response factors		50	36.6 ± 0.4

3.7 X-Ray Photoelectron Spectroscopy Analysis:

Different methods were studied for plasma polymer characterization as discussed in Chapter 1. X-Ray Photoelectron spectroscopy (XPS) was chosen because it is a powerful technique for analysis of surfaces and is suited for determination of the chemical character of such films. The information available from the technique includes semiquantitative elemental analysis, functional group identification dependent on electronegativity of nearest neighbor atoms, and depth profiling which is not available in other techniques.

XPS was performed with a KRATOS AXIS XPS instrument, shown in Figure 9. Monochromatised AL Ka radiation (148.7 eV) was used for photo electron excitation. The analyzer pass energy was kept constant at 40 eV for the high resolution scans by NRC's Environmental Protection Science group. XPS analysis was done on different samples of dry aluminum foil as well as on aluminum foil plasma treated with aniline.

A depth profile was accomplished by etching each sample's surface with an argon ion gun.

Charge neutralization, necessary due to the positive charge accumulation at the surface of the non conducting SPUs, was achieved using a low energy (0-20 eV) electron flood gun.

High resolution spectra were deconvoluted by means of computer assisted-fitting techniques. Peak areas were subsequently integrated and normalized according to atomic sensitivity factors and referenced to the CH_x peak maximum at 285.0 eV.

All spectra were obtained under a pressure of approximately 10^{-8} torr.

3.7.1 X-Ray Photoelectron Spectroscopy System

Figure 16 shows a schematic representation of an XPS system. Mg Kα radiation is used in most instruments. The emitted electrons must pass through an energy "window" in the analyzer to reach the detector and be counted. Only those electrons with a KE which falls within the range of the window (determined by the pass energy) are accepted. The pass energy can be varied, and must reflect a compromise between the conflicting requirements of good resolution (low pass energy) and an acceptable intensity (high pass energy), both within a reasonable length of time.

The sampling chamber is kept at ultra high vacuum (UV) at all times to minimize both the scattering of emitted photoelectrons and the accumulation of surface contamination by residual gas in the vacuum system. Typical pressures are in the 10^{-8} to 10^{-11} torr range.

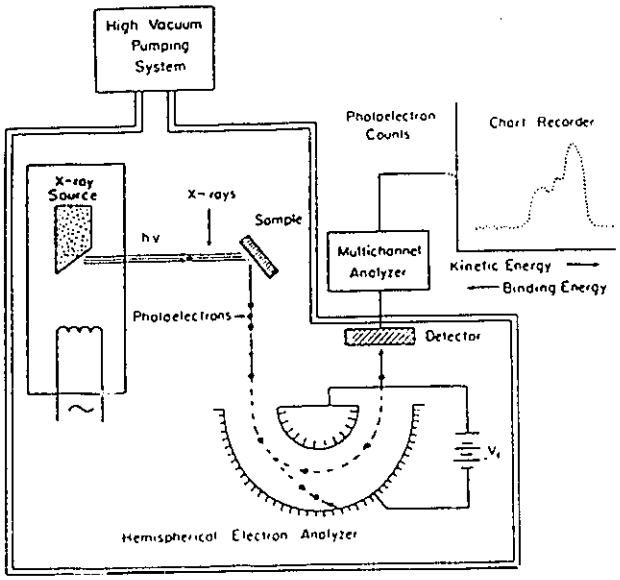

Figure 16: Schematic diagram of an XPS system (Ratner, 1986)

Chapter 4

Results and Discussion

4.1 Plasma Treatment

The plasma treatment was performed in the presence of aniline vapor using the following conditions:

Argon flow rate: 10 cm^3 (STP)/min.

Pressure of plasma chamber: 0.88 Pa (0.15 mtorr).

- Power: 75 W.
- Frequency: 13.56 MHz.
- Exposure time: 15 min.

Many trials were required to determine the above optimum conditions. Pressure and frequency were maintained at 0.88 Pa and 13.56 MHz respectively. Conditions for power, time and flow rate were varied as follows:

- Power: 25, 50, 75 and 100 W.
- Exposure time: 5, 10, 15, 20 and 25 min.
- Argon flow rate: 4, 6, 8, 10 and 12 cm^3 (STP)/min.

Various combinations, of the above conditions were tried based on information obtained from a literature survey reported in Table 1. Many combinations of these conditions resulted in powder instead of a thin film of plasma so the results were not recorded.

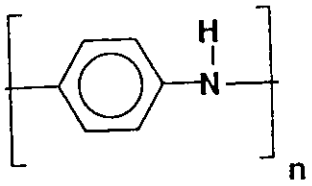

POLYANILINE

4.2 Surface Characterization Using X-ray Photoelectron Spectroscopy

X-ray Photoelectron Spectroscopy (XPS) analysis of an aluminum foil sample without any treatment was done. The analysis showed the presence of oxygen, aluminum, carbon, silicon and magnesium on the surface. Three different areas of the sample (size 10^{-3} mX 10^{-3} m) were subjected to the XPS analysis to ensure that the surface chemistry of the sample was uniform. The results of the analysis are summarized in Table 4. The data given as atomic concentrations are quite consistent for three spots. The data shows the high atomic concentration of aluminum, which is quite natural. The presence of high carbon concentration is probably due to the contamination of the surface called adventitious carbon which is a phenomenon often observed for metal surfaces. Oxygen was also detected in a high concentration. The oxygen may be from aluminum foil, the

basic structure of which is aluminum oxide, or it may be from water. The XPS signals are presented in Figure 17.

Table 4: XPS analysis of untreated aluminum foil

Surface Content		Atomic Concentration %			
Spot Number		2	3	4	Average
Total Carbon		13.60	14.53	14.57	14.28
Functional Group	BE (eV.)				
C-C	285.0	8.77	8.42	8.34	8.51
C-O or C-N	287.2	3.08	3.61	4.02	3.57
C=O or C=N	289.7.	1.75	2.50	2.21	2.20
Total Oxygen		52.40	52.16	52.73	52.40
Total Aluminium		33.82	33.03	32.52	33.10
Total Magnesium		0.18	0.28	0.19	0.20
Silicon	Only very small trace				

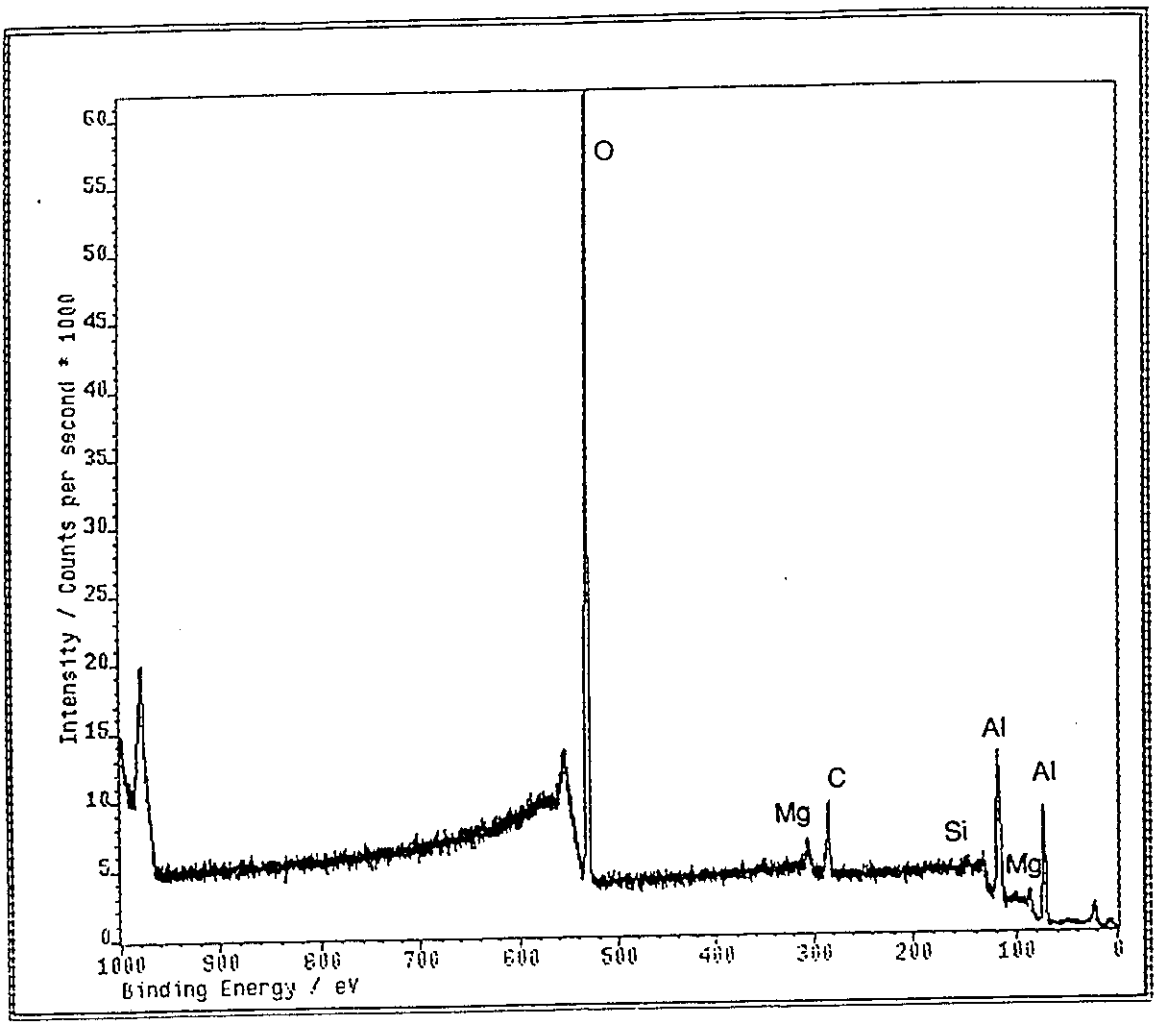

Figure 17: XPS analysis for a blank aluminum foil

XPS analysis was also conducted after plasma treatment of the sample (Figure 18). This Figure shows that XPS signals corresponding to carbon, oxygen and nitrogen were found. The oxygen and nitrogen are single peaks whereas the carbon can be deconvoluted into three distinct peaks located at 285.0 eV, 287.2 eV and 289.7 eV. The results were further summarized in Table 5 & 6 for two different samples. The difference between the two samples is that the sample corresponding to Table 5 was kept in the plasma chamber under vacuum over a weekend after the plasma coating was completed, and then the chamber was opened and the sample was exposed to air. The sample corresponding to Table 6 on the other hand, was exposed to air immediately after the completion of plasma coating. The Tables include data for three different spots and their average. Table 6 also includes theoretical values of atomic concentrations calculated from the structure of polyaniline.

Several conclusions can be drawn from these two tables. The theoretical oxygen content in polyaniline is supposed to be zero, but in both Table 5 and 6 significant amounts of oxygen are found. This was probably due to the reaction of aniline radicals with oxygen when the plasma coated sample was exposed to air. The oxygen content in Table 5 is lower than that in Table 6 which means that some aniline radicals disappeared while being stored under vacuum over a weekend. Another conclusion is that the experimental results agree with theoretical polyaniline except oxygen was present with the experimental values.

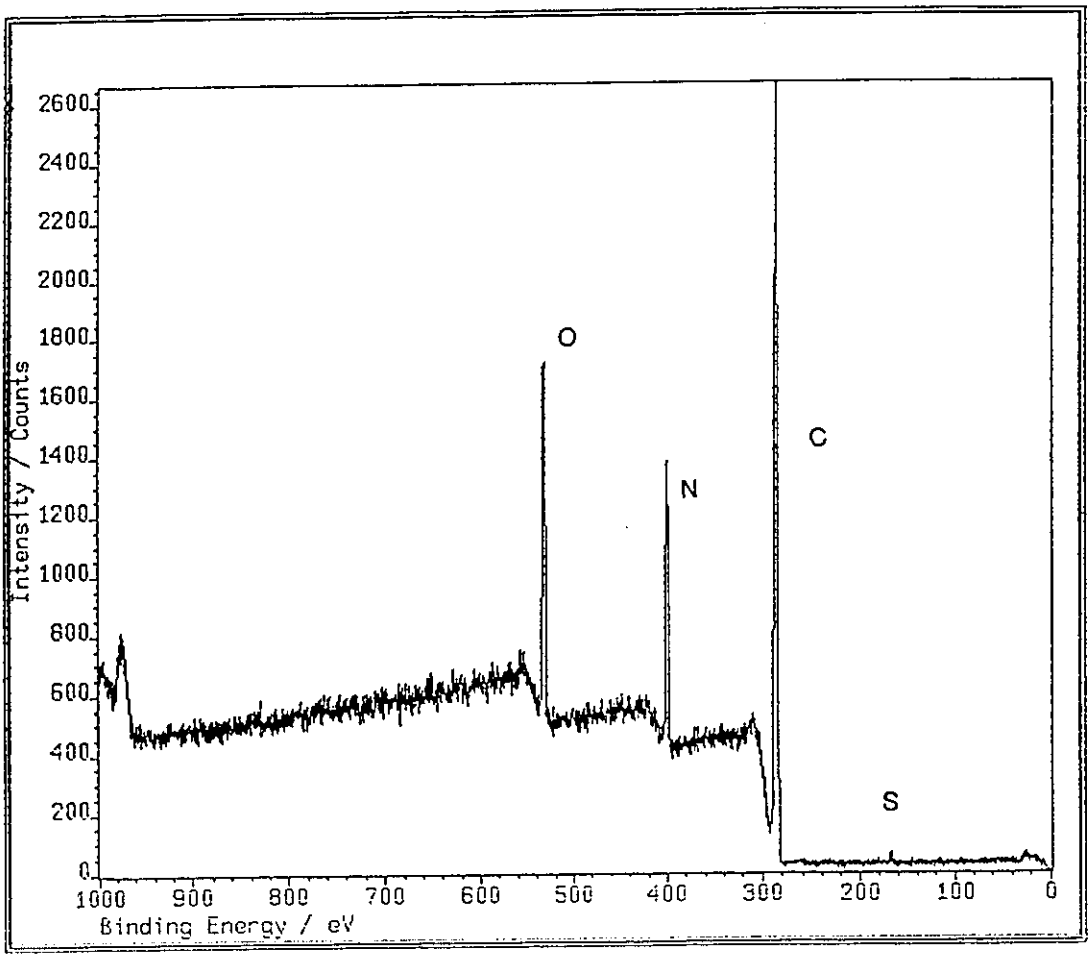

Figure 18: XPS analysis for aniline plasma deposited on aluminum foil

Table 5: XPS analysis of treated aluminium foil with aniline plasma

Surface content		Atomic concentration %			
Total carbon		77.13	77.31	76.48	76.9
Functional Group	BE (eV.)				
C-C	285.0	51.16	54.54	51.11	52.3
C-O or C-N	287.2	21.89	19.56	20.93	20.86
C=O or C=N	289.7	4.08	3.21	4.44	3.90
Total Oxygen		9.56	9.63	9.97	9.70
Total Nitrogen		13.30	13.06	13.55	13.30

Table 6: XPS analysis of aniline plasma deposited on aluminum foil compared to the theoretical polyaniline.

Surface content	Atomic Concentration					
					Average	Theoretical Polyaniline
Total carbon		71.12	71.65	70.92	71.20	85.70
Functional Group	BE (eV.)					
C-C	285.0	37.25	38.87	39.54	38.80	57.10
C-O or C-N	287.2	27.46	26.02	26.28	26.6	28.60
C=O or C=N	289.7	6.41	6.76	5.10	6.1	0.00
Total Oxygen		15.04	14.30	14.36	14.60	0.00
Total Nitrogen		13.85	14.04	14.73	14.20	14.30

The sample surface was etched with an argon ion gun in an attempt to obtain a depth profile. Table 7 summarizes the results of six one minute etches and a final 5 minute etch. The table indicates that no aluminum signal was observed even after eleven minutes of etch. This could suggest that polyaniline film was deposited as a continuous separate layer on top of the aluminum foil sample. Oxygen content originally decreased 15 % to 10% (see Tables 5 and 6) to 2.1 % after one minute etch and further decreased to

1.0 to 1.4%. This suggests that oxidation of radicals took place primarily at the top surface of the polymer layer. Etching also decreases the nitrogen from almost 14% to 10% in the first etch. This means that polyaniline plasma deposited on the surface of the sample is not homogeneous throughout the layer.

Table 7: XPS analysis with various etch times

			Composition in atomic %						
Etch time (minutes)		0	1	2	3	4	5	6	11
Total Carbon		71.12	87.7	90.4	91.7	91.95	92.7	92.2	91.8
Functional Group	BE (eV.)								
C-C	285.0		59.1	58.6	67.2	60.4	65.5	64.2	58.5
C-O or C-N	286.2		22.0	20.3	12.6	21.5	18.2	17.9	21.3
C-O or C-N	288.0		6.5	7.2	7.5	6.3	5.6	6.8	7.5
C=O or C=N	290.1		4.2	4.3	4.1	3.7	3.4	3.2	4.5
Total Oxygen		15.04	2.1	1.8	1.7	1.1	1.0	1.2	1.4
Total Nitrogen		13.85	10.2	7.9	6.9	7.0	6.3	6.6	6.9
Al		0.0	0.0	0.0	0.0	0.0	0.0	0.0	0.0

The plasma coated aluminum foil sample was further analyzed by angle resolve (tilting the sample). The larger the tilt angle, the shallower was the penetration. The results are summarized in Table 8. The data for oxygen and nitrogen contents do not change much with a change in tilt angle. This means that the oxygen and nitrogen were uniformly distributed within the top 75 to 100 Å. This suggests that the thickness of the

polymer layer is much more than 75 Å. We do not know the etching rate of the argon ion gun but it is likely 75 Å/minute for organic materials. However, the individual functional groups do show a change in concentration as the tilt angle changes. The C-C hydrocarbon peak (BE 285.0 eV.) shows a gradual decrease in concentration as the tilt angle (and sampling depth) increases, while the C-O, C-N functionalities (BE 287.2 eV.), and the C=O, C=N functionalities (BE 289.3 eV.) show a steady decrease in concentration as the tilt angle increases. This suggests that there is a surface enrichment of the carbon, oxygen and carbon/nitrogen groups over the carbon/carbon substrate. This enrichment shows that there are slight chemical changes taking place within the top 100 Å of the material, even though the total concentrations of oxygen and nitrogen remain the same.

Table 8: Analysis with different tilt angle

Surface content	Composition in atomic %			
Angle resolve analysis		0° tilt	60° tilt	75° tilt
Total carbon				
Functional Group	BE (eV.)	71.2	72.8	73.6
C-C	285.0	38.8	48.5	59.9
C-O or C-N	287.2	26.6	19.7	13.7
C=O or C=N	289.3	6.1	4.6	0.0
	Total oxygen	14.6	13.9	12.5
	Total nitrogen	14.2	13.9	13.9

4.3 Pure Gas Permeation Experiments

Pure gas permeation experiments were performed to study the permeability of helium, hydrogen, carbon dioxide, oxygen, nitrogen and methane gases with coating time. The permeation cells used for the experiment, the experimental procedure and the experimental conditions were described in detail in Chapter 3. Permeation rates were recorded every 15 minutes after the start of the permeation experiment and the data were averaged. Normally, the standard deviation of the permeation data was $\pm$ 5 %. The permeability data are shown in Table 9 and in Figures 19 a and 19 b for six gases as a function of the plasma coating time. They show the decrease in permeability from zero to ten minutes of plasma coating time. The permeability then increases from ten to twenty minutes and decreases again from twenty to twenty five minutes. This change in the shape is probably due to the interaction of two phenomena, one is the increased thickness of the coated layer and the other is increased disruption of the substrate.

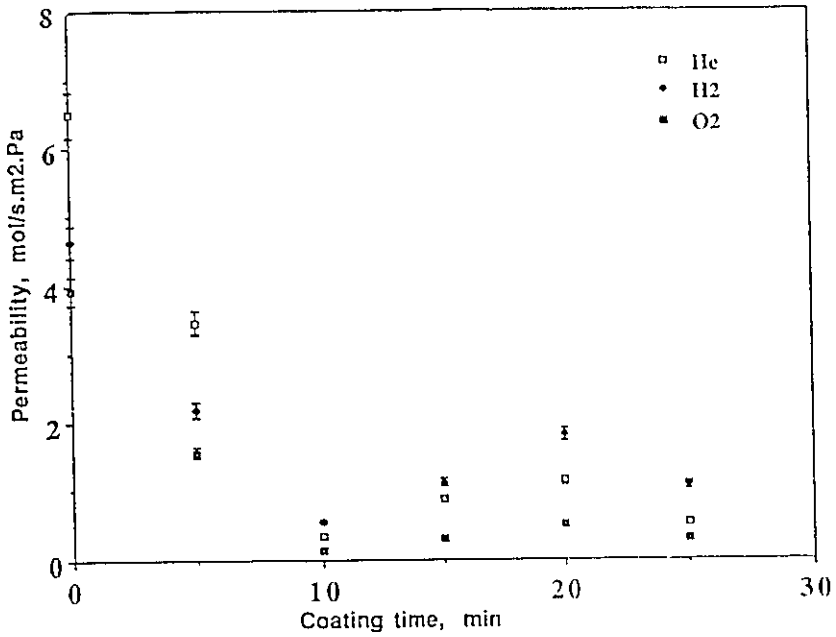

Figure 19 a: Gas permeabilities through uncoated and coated membrane

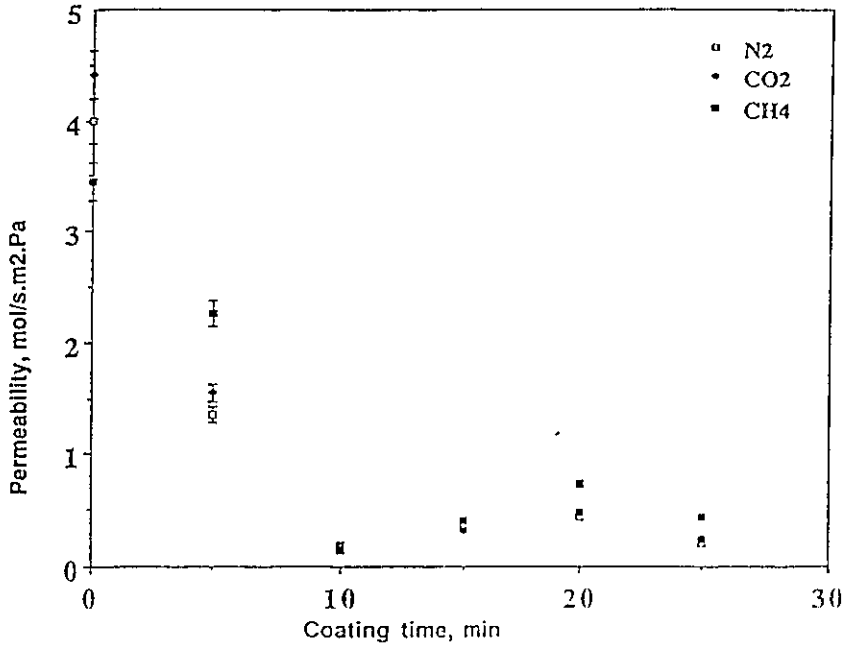

Figure 19 b: Gas permeabilities through uncoated and coated membrane

Table 9: Variation of gas permeability of aniline plasma coated PES membranes with coating time

Gas	(Gas Permeability)x10^7, mol/s.m^2.Pa					
	uncoated	5 min., Coating	10 min., Coating	15 min., Coating	20 min., Coating	25 min., Coating
He	6.50	3.44	0.35	0.88	1.14	0.53
H_2	4.63	2.18	0.55	1.11	1.81	1.07
O_2	3.92	1.54	0.14	0.30	0.51	0.29
N_2	4.00	1.35	0.14	0.34	0.43	0.20
CO_2	4.41	1.55	0.15	0.32	0.48	0.25
CH_4	3.45	2.26	0.19	0.40	0.72	0.43

4.4 Pure Gas Permeation Rate

Table 10 shows the variation of pure gas permeation rate ratios with the plasma coating time. The permeation rate ratio is defined as the ratio of permeability of helium gas to that of a given gas. The permeation rate ratio for helium is therefore always unity. Regarding the permeation rate ratio of gases whose molecular weights are greater than that of helium (O_2, N_2, CO_2, and CH_4), the permeation rate ratios show a definite pattern; i.e. there is a maximum at 15 minutes of plasma coating time. Only nitrogen gas is exceptional, and the ratio continues to increase as the coating time increases. The increase is, however, rather marginal. Interestingly, the permeation rate ratios at 15 minutes coating time are close to those calculated by assuming the Knudsen flow mechanism; i.e. experimental values are 0.8, 2.9, 2.6, 2.8 and 2.2, whereas theoretical values are 0.7, 2.8, 2.6, 3.3 and 2.0, respectively, for H_2, O_2, N_2, CO_2 and CH_4. From these data we can conclude that both viscous flow and Knudsen flow are occurring in membranes whose coating times are different from 15 min. On the other hand, the Knudsen flow dominates in the pores of the membrane with 15 minutes coating time. Pore sizes of the plasma coated membranes are, therefore, too large for any significant gas separation to take place. It should be noted however, that selectivities higher than the value expected from the Knudsen mechanism (or the pure gas permeation rate ratio lower than the Knudsen mechanism) was obtained for hydrogen gas.

Table 10: Variation of permeation ratio with plasma coating time

Time (min.)	He	H_2	O_2	N_2	CO_2	CH_4
0	1.0	1.4	1.7	1.6	1.5	1.9
5	1.0	1.6	2.2	2.5	2.2	1.5
10	1.0	0.6	2.5	2.5	2.3	1.8
15	1.0	0.8	2.9	2.6	2.8	2.2
20	1.0	0.6	2.2	2.7	2.4	1.6
25	1.0	0.50	1.8	2.7	2.1	1.2

4.5 Separation of Gas Mixtures

Mixtures of carbon dioxide /methane with three different compositions were separated by a polyethersulfone substrate laminated with a silicon rubber layer. The preparation of the membrane, the experimental procedure and the conditions of the separation experiments are described in detail in Chapter 3.

Tables 11 a, 11 b and 11 c show variations in the permeate mole fraction, the separation factor and the permeate flux with an increase in the CO_2 mole fraction in the feed. The data show an increase in the separation factor as well as the flux with an increase in the feed CO_2 mole fraction.

Table 11 a: Composition of carbon dioxide and methane in feed and product

Feed mole fraction		Permeate mole fraction	
CO_2	CH_4	CO_2	CH_4
0.00	1.00	0.00	1.00
0.25	0.75	0.79	0.21
0.50	0.50	0.92	0.09
0.75	0.25	0.96	0.04
1.00	0.00	1.00	0.00

Table 11.b: Values of separation factors through laminated polysulfone for carbon dioxide and methane

Feed, mole fractions CO_2: CH_4	Separation Factor, α
0.25: 0.75	11.0
0.50: 0.50	12.6
0.75: 0.25	14.0

$$\alpha = \frac{\left(CO_2 \text{mole fraction} / CH_4 \text{ mole fraction}\right)_{\text{permeates}}}{\left(CO_2 \text{mole fraction} / CH_4 \text{mole fraction}\right)_{\text{feed}}}$$

Table 11.c: Values of flux through laminated polysulfone membrane for carbon dioxide and methane mixture

Feed fractions, CO_2: CH_4	Flux, $(mol/m^2 \cdot s) \times 10^4$
0.25: 0.75	4.07
0.50: 0.50	6.52
0.75: 0.25	12.25

4.6 Resistance Model Analysis

The modified resistance model approach was used to analyze the gas permeation data for PES membranes laminated with SR (Silicon Rubber) membrane. As noted previously in Chapter 2, it was necessary when applying the resistance model, to use the parameter (α_2), defined by equation (16) for the substrate membrane (PES). The values for (α_2) for PES membrane were taken from the intrinsic permeability values in the literature (Kumazawa and Wang, 1993; Aitken et al., 1992), for CO_2/CH_4 and O_2/N_2, which were 32.2 and 3.2 respectively shown in (Appendix B). In the case of plasma coated PES there were no comparable literature values for the intrinsic permeability of different gases in this material.

The following section discusses the results of the resistance model analysis applied to the permeation data of pure gas components of two gas mixtures, namely CO_2/CH_4 and O_2/N_2 at a constant feed pressure of 758 kPag.

4.6.1 Resistance Model Analysis for Laminated PES Membranes

Table 12 shows the experimental permeability data for O_2, N_2, CO_2 and CH_4 gases in PES before and after lamination with SR. The table also contains the data for the component resistance calculated from the permeability data.

The overall resistance for all gases increased significally after lamination which was expected due to the increase in the total resistance after adding the laminating layer. However the O_2/N_2 permeability ratio increased from 0.98 before lamination to 3.17 after

lamination. The same phenomena was observed for the CO_2/CH_4 gas mixture. While the overall resistance (R_t) increased dramatically after lamination for both CO_2 and CH_4 gases, the CO_2/CH_4 permeability ratio increased from 1.28 to 23.71.

Before lamination, the gas flow is primarily controlled by the pore resistance (R_3), since it is much smaller than the polymer matrix resistance (R_2). In this case we would expect that Knudsen flow would be the dominating flow mechanism for different gases resulting in a low selectivity. However, by examining the component resistance values presented in Table 12, we can see that for the laminated membranes, the resistance R_1' for the portion covering the pore area is much higher than the resistance R_1 for the portion covering the polymer matrix. This means that after lamination most of the gas would flow through R_1+R_2 branch rather than flowing through $R_1'+R_3$ branch. For this reason, the permeability ratio after lamination would approach the value of the intrinsic permeability ratio of CO_2/CH_4 and less Knudsen flow would occur in the laminated membrane as compared with the membrane before lamination. All the resistances calculated in table 12 are based on assigned value of errors that was set to be 1.0.

Table 12: Permeability and Resistance data for PES membranes at pressure 758 KPa

	O_2	N_2	CO_2	CH_4
Gas Permeability before lamination (mol/s.m^{2}Pa)	0.415E-06	0.424E-06	0.467E-06	0.365E-06
Gas Permeability after lamination (mol/s.m^2.Pa)	0.374E-09	0.118E-09	0.275E-08	0.116E-09
Resistance (Pa.s/mol)				
R_1	0.237E12	0.473E12	0.438E11	0.148E12
R_1'	0.101E16	0.201E16	0.822E14	0.277E15
R_2	0.128E13	0.854E13	0.336E12	0.915E13
R_3	0.251E10	0.245E10	0.224E10	0.284E10
R_t	0.251E10	0.245E10	0.223E10	0.284E10
R_t^L	0.278E13	0.882E13	0.378E12	0.899E13

4.7 Gas Permeability Data for PES Membranes Coated then Laminated

Table 13 shows the gas permeability for CO_2, CH_4, O_2 and N_2 gases in PES plasma coated membranes before and after lamination. During the plasma coating large pores are created. When silicone rubber is added to the plasma coated membrane the order is reversed because silicone rubber is more permeable to nitrogen than oxygen.

Table 13: Gas permeability of membranes PES plasma coated and then laminated

Gas Permeability ($mol/m^2.Pa$)	CO_2	CH_4	O_2	N_2
PES Plasma coated	0.164E-06	0.163E-06	0.163E-06	0.143E-06
PES Plasma coated and laminated with silicon rubber	0.250E-08	0.280E-08	0.190E-08	0.380E-08

Chapter 5

Conclusions

1. Surface characterization using x-ray photoelectron spectroscopy shows that:
    a) there is a deposition of a layer 75-100Å.
    b) experimental and theoretical results of the deposition process agree except for the presence of oxygen.
    c) oxygen on the plasma coat could come from the reaction of air with the aniline radicals
2. Pure gas permeation of six gases (He, H_2, CO_2, O_2, N_2 and CH_4) through plasma coated PES with coating time from 0 to 25 minute shows that increasing the coating time changes permeability because of the interaction of two effects:
    a) the increased disruption of the substrate
    b) the increased thickness of the coating layer
3. The experimental values of the pure gas permeation ratios after 15 minutes coating for all gases except N_2 are close to those calculated by assuming the Knudsen flow mechanism. Both viscous flow and Knudsen flow occur in membranes whose coating times are different from 15 minutes.

4. Pore sizes of the aniline plasma coated membranes are too large for any significant gas separation to take place.

5. Laminated PES membranes were effective in separating a mixture of CO_2 and CH_4. An increase in feed CO_2 shows an increase in the separation factor and the flux.

6. The modified resistance model indicates that less Knudsen flow occurs in the laminated membrane with silicon rubber as compared with the membrane before lamination.

Chapter 6

Recommendations

Care must be taken when choosing the substrate membranes i.e. small pore size to improve the selectivity. Another solution could be to redesign the gas inlet inside the plasma chamber in order to achieve even distribution of the plasma coat on the membranes.

Bibliography

Aitken, C. L., W. J. Koros and D. R. Paul, "Gas Transport Properties of Biphenol Polysulphones", Am. Chem. Soc. **25** (14), 3651 (1992).

Anand, M., R. E. Cohen and Baddour, "R.F", Polym., **22**,361 (1981).

Arquette G. J., "Insolubilization of Coatings", U.S. Patent **3, 061, 458** (1962).

Austin, J. B. and I. A. Black, "The Chemical Behavior of Some Benzoid Hydrocarbons in the Tesla Discharge", J. Am. Chem. Soc., **52**, 4552 (1930).

Barrer, R. M. , J. A. Barrie, and J. Slater, "Sorption and Diffusion in Ethyl Cellulase. Part III. Comparison Between Ethyl Cellulose and Rubber", J. Polym., Sci., **27**, 177 (1958).

Biederman, H., S. M. Ojha and L. Holland, "The Properties of Fluorocarbon Films Prepared by r.f. Sputtering and Plasma Polymerization in Inert and Active Gas", Thin solid Films., **41**, 329 (1977).

Bradley, A. and J. P Hammes, "Electrical Properties of Thin organic Films", J. Electrochem. Soc., **110**, 15 (1963).

Cai, S., Y. Xuehai and F. Jinglin, "Gas Permeability of Plasma-Polymerized Organosiloxane Composite Membranes", Mo Kexue Yu Jishu, 9 (3), 8, (1989).

Canepa, P. , M. Nicchia, S. Munari and G. Bena "Use of Nuclepore Film in the Synthesis of Membranes for Gas Separation", Chim. Ind. (Millan) ,**66** (4), 238 (1984).

Chang, F. Y., M. Shen and A.T. Bell, "Composite Permselective Membrane by deposition of an Ultrathin Coating from a Plasma", J. Appl. Polym. Sci. **17**, 2915 (1973).

Coleman, J. H., "Polymerization Method And Apparatus", U.S. Patent, **3, 068, 510** (1962).

DeNaylor, V. T., "Permeation Properties" Comprehensive Polym. Sci.: The Synthesis, Characterization, Reactions & Applications of Polymers, 2 (C) Pergamon, (1989).

Dietz, W. A., "Response Factors for Gas Chromotographic Analysis", J. Gas Chromotography **15**, 68 (1967).

Dilks, A.and S. Kaplan, "X-ray photoelectron Spectroscopy for the Investigation of Polymeric Materials", Proc. Symp. Plasma Process 3rd, **31**, 82 (1981).

Frisch, H. L. , D. Klempner, and T. Kwei, "Modified Free Volume Theory of Penetrant Diffusion in Polymers", Macrom. **4**, 237 (1971).

Fujita, H. "Diffusion in Polymer Diluent Systems", Fortschr. Hochpolym. Forsch. **3** (1) (1961).

Fujita, H., "Organic Vapors Above the Glass Transition Temperature. In Diffusion in Polymers", ed. J. Crank and G. s. Park. New York: Academic Press (1968).

Fujita, H. , A. Kishimoto, and K. Matsumoto "Concentration and Temperature Dependence of Diffusion Coefficients for Systems Polymethyl acrylate and n-alkyl acetates", Trans. Farady Soc. **56**, 424 (1960).

Goodman, J., J. "The Formation of Thin Polymer Films in the gas Discharge" Polym. Sci. **44**, 551 (1960).

Grenda, M.S. and M. Venugopalan, "ESR Signal of Polymer Prepared In Situ in Xylene Plasma", J. Polym. Sci. **18**, 1611 (1980).

Haggin, J., "New Generation of Membranes Developed for Industrial Separation" C & Eng. Chicago, 7, June, (1988).

Harkins, W. B. and J. M. Jackson, J., "A Spectroscopic Study of the Decomposition and Synthesis of Organic Compounds by Electrical Discharges: Electrodeless and Glow Discharges", Chem. Phys., **1**, 37 (1933).

Hasumi, K , K. Murata, O Yoshiyuki and O Yoshuki, "Polymer Membranes with High Capacity in Gas Separation", Jpn. Kokai Tokkyo Koho, 8 pp (1987).

Havens, M.R., K.G. Mayhan and W.J. James, "Plasma Deposited Polymer Films. II Transmission and Scanning Electron Microscopy", J. Appl. Polym. Sci., **22**, 2799 (1978).

Havens, M.R., K.G. Mayhan and W.J. James, "Plasma-Deposited Polymer Films. I. Low Angle X-Ray Study", J. Appl. Polym. Sci., **22**, 2793 (1978).

Henis , J. M. S. and M. K. Tripodi, "Multicomponent Membrane For Gas Separation", U.S. Pat. **4, 230, 463**, Oct. 28, (1980 b).

Henis, J. M. S. and M. K. Tripodi, "A Novel Approach to Gas Separation Using Composite Hollow Fiber Membranes", Sep. Sci. Tech. **15**, 1059-1068 (1980 a).

Heffernan, P., K. Yanagihara, Y. Matsuzawa, E. E. Hennecke, E. W. Hellmuth, H. Yasuda, "Preparation and Characterization of Composite Hollow fiber Reverse Osmosis Membranes by Plasma Polymerization. 1. Design of Plasma Reactor and Operational Parameters", Ind. Eng. Chem. Prod. Res. Dev., 23(1), 153-62 (1984).

Hirota K. and N. Aihiro, "Fluro or Siloxane Copolymer Membrane and its Manufacture", Jpn. Kokai Tokkyo Koho, 4 pp., (1991).

Hirotsu, T., "Water-Ethanol separation by Pervaporation Through Plasma Graft Polymerized Membranes", J. Appl. Polym. Sci., **34** (3), 1159 (1987).

Hirotsu, T. and M. Isayama, "Water Ethanol Separation by Pervaporation through Plasma-Graft -Polymerized Membranes of 2-hydroxyethyl Methacrylate with Acrylic Acid or Methacrylic acid", J. Membr. Sci., **45** (1-2), 137 (1989).

Hirotsu, T. and S. Nakajima, "Water-Ethanol Permseparation by Pervaporation through the Plasma Graft Copolymeric Membranes of Acrylic acid and Acryamide", J. Appl. Polym. Sci., **36** (1) 177 (1988).

Hirotsus, T and A, Arita, "Plasma Graft Polymerization of N, N-dimethylaminoethyl methacrylate and Water -Ethanol Separation by Pervaporation Through the Grafted Membranes", J. Appl. Polym. Sci. **42** (12) 3255 (1991).

Hollahan, J. R. and T. Wydeven, "Some Experimental Parameters Affecting Performance of Composite Reverse Osmosis Membranes Produced by Plasma Polymerization", J. Appl. Polym. Sci., **21**, 923 (1977).

Inagaki, N. and H. Katsuoka, "Gas Separation Membranes Made by Plasma Polymerization of Mixtures of Silanes and Fluromethane", J. Membr. Sci., **34** (3), 297 (1987).

Kaplan, S. and A. Dilks, "Characterization of Plasma-Polymerized Materials by Modern Spectroscopic Techniques", J. Appl. Polym. Sci., Appl. Polym. Sym. (JPSSDD), **38**, 105 NY (1984).

Kaplan, S. and A. Dilks, "Solid State Nuclear Magnetic Resonance Investigation of Plasma-Polymerized Hydrocarbons", Thin Solid Films, **84**, 419 (1981).

Kashiwagi, T., O. Kazuhiro and O. Koichi, "Manufacture of Pervaporatio Membranes for Separation of Liquid Mixtures", Jpn. Kokkyo, 4 pp. (1988).

Kawakami, M., Yamashita, Y. I. Masakazu and K. Shuichi, "Modification of Gas Permeabilities of Polymer Membranes by Plasma Coating", J. Membr. Sci., **19** (3), 249 (1984).

Kobayashi, H, M. Shen, "Effects of Monomer Flow Rate, Flow Configuration, Reactor Geometry on the Rate of Plasma Polymerization", J. Macromol.Sci., **10**, 491 (1976).

Kobayashi, H., M. Shen and A.T. Bell, "Effect of Reaction Conditions on the Plasma Polymerization of Ethylene", J. Macromol. Sci. **8**, 373 (1974).

Koichi, O.and S. Asako, "Selectively Gas-Permeable Composite Membrane", Eur. Pat. Appl., 25 pp. (1983).

Kramer, P. W. and and H. Yasuda "Effect of Operational parameters on the Air Separation Properties of Composite Hollow Fiber Membranes Prepared by Plasma Polymerization of Perfluorodimethylcyclobutane", . Polym. Sci., **42**, 381 (1988).

Kumazawa, H., J.-S. Wang and E. Sada, "Gas Transport Through Homogeneous and Asymmetric Polyethersulphone Membranes", J. Polym. Sci. Part B Polym. Phys., **31**, 881 (1993).

Linder, E. G. and A. P Davis. "Reactions of Hydrocarbons in the Glow Discharge" J. Phys. Chem., **35**,3649, (1931).

Loeb, S. and S. Sourirajan, "Sea Water Demineralization by means of a Semipermeable Membrane", Report No. **6060**, UCLA (1960).

Matsuura, T., Y. Chen and T. Okada, "Science of Membrane Transport and Membrane Design", In North American Membrane Society, Inc. 3rd annual meeting, May (1989).

Masuoka T., K. Mizoguchi, O., Hirasa and M. Suda, "Manufacture of Liquid-Separating Membranes for Selective Separation of Ethanol", Jpn. Kokai Tokkyo Koho, 3 pp., (1987).

McHattie, J S., "Effect of Structural Modifications on the Gas Transport Properties of Polysulfones and Polycarbonates", Ph D. Thesis. The University of Texas at Austin (1990).

Micheals, A. S., W. R. Vieth, and J. A. Barrie. "Diffusion and Solution of Gases in Poly(ethylene terephthate)", J. Appl. Phys , **34** (1), 13.(1963).

Minhas, B.S., T. Matsuura, and S. Sourirajan, "Formation of Asymmetric Cellulose Acetate Membranes for the Separation of Carbon dioxide-Methane Gas", Ind. Eng. Chem. Res., **26**, 11, 2344 (1987).

Mohammadi, T. A, "Ph. D. Thesis, to be published, University of Ottawa, Ont., Canada (1994).

Morinaka, A. and Y. Asano, "Residual Stress and Thermal Expansion Coefficient of plasma Polymerized Films", J. Appl. Polym. Sci., **27**, 2139 (1982).

Morita, S., T.Mizutani and M. Ieda, "Electron Spin resonance in Thin Polymer Films by the Thin polymer Films by the Glow Discharge Indirect Method", J. Appl. Phys., **10**, 1275 (1971).

Morosoff, N., D. L. Patel, A.R. White, M. Umana, D.B. Brown, A.L. Grumbliss and P.S. Lugg, "Plasma Polymerization of Iron Pentacarbonyl with C_2 Hydrocarbons", Thin Solid Films, **117**, 1, 33 (1984).

Morosoff, N., R. Haque, S. D. Clymer and A.L. Crumbliss, "Transition Metal Containing Plasma Polymers", J. Vac. Sci., Technol., A3, 2089 (1985).

Nakamura, S., S. Yamanake, Y. Yamaguchi and G. Sawa, "The Correlation of transient Electric Current With Free Radicals in Plasma Polymerized Styrene, J. Appl. Phys., **19**, 777 (1980).

Nomura, H., P. W. Kramer and H. Yasuda, "Preparation of Gas Separation Membranes by Plasma Polymerization with Fluro Compounds", Thin Solid Films **118** , 187 (1984).

Okita, K., "Gas- Permselective Composite Membranes", U.S. 382 (1985).

Okita, T., Y. Shinichi, A. Shigeru and K. Yamada, "Liquid Membrane", Eur. Pat. Appl., 26 pp. (1986.)

Otazai, K., Kume S. Nagai S. Yamamoto T., And Fukushima S.Bull, "Polymerization by Electric Discharge", Chem. Soc. Jpn., **2727**, 476 (1954).

Pavia, D., G. Lampman and G. Kriz, "Introduction to Organic Laboratory Techniques", second edition, 517 (1982).

Ratner, B. D., "In Spectroscopy in the Biomedical Sciences", CRC Press, Boca, Fla 107 (1986).

Raucher, D., and M. D. Sefcik, "Gas Transport and Cooperative Main Chain Motions in Glassy Polymers", In ACS Symp. Ser. No. 233, Industrial Gas Separations ed. T. E. Whyte, C. M. Yon, and E. H. Wagener, Washington, DC: American Chemical Society, (1983 a).pp. 111-124.

Raucher, D., and M. D. Sefcik, "Sorption and Transport in Glassy Polymers", In ACS Symp. Ser. No. 233, Industrial Gas Separations ed. T. E. Whyte, C. M. Yon, and E. H. Wagener, Washington, DC: American Chemical Society (1983 b). pp. 111-124

Sada, E, H. Kumazawa, P. Xu and Inoue "Transport of a Gas Through Asymmetric Polysulfone Membranes with Deposited Plasma Polymerized Thin Layer", J. Appl. Polym. Sci., 41 (9-10), 2427 (1990).

Sakata, J., M. Yamamoto, and M. Hirai, "Plasma-Polymerized Membranes and Gas Permeability II" J. Appl. Polym. Sci., **31**, 1999, (1989).

Sakata, J., Y. Minoru and H. Masana "Effect of Plasma Polymerization Conditions on Gas Permeability of Plasma-Prepared Films", Kobunshi Ronbunshu, **45** (6) 499 (1988).

Samejiima, S. and H. Nakamura, "Membranes for Separation of Helium from Natural Gas", Jpn. Kokai Tokkyo Koho, 3 pp. (1987).

Saruyama, T., "Plastic Membranes for Oxygen Enrichment", JP Kokai Tokkyo Koho (1991).

Schoepfle, C. S. and L. H. Connel, "Effect of Cathode Rays on Hydrocarbon Oils and on Paper", Ind. Eng. Chem., **21**, 529 (1929).

Scott, T. W., K. C.Chu and M. Venugopalan, "ESR Signal of Polymer Film Formed in Xylene Plasma", J. Polym. Sci., **17**, 267 (1979).

Seeger, M., E.M. Barra II and M. Shen, "Pyrolysis and Gas Chromatography of Plasma-Polymerized Ethylene", J. Polym. Sci., **13**, 1541 (1975).

Seeger, M., R.J. Gritter, J.M. Tibbitt, M. Shen, and A.T. Bell, "Analysis of Plasma-Polymerized Hydrocarbons by Pyrolysis/Gas Chromatography", J. Polym. Sci., **15**, 1403 (1977).

Song, R., S. yue, J. Liu, J. Chen, Z. Chen and X. Liu, "ESR Studies of Plasma Polymerized Tetrafluroethylene", Gaodeng Xuexias Huaxue Xuebao, **4**, 139 (1983).

Spillman, R. w., "Economics of Gas Separation Membranes", Chemical Engineering Progress, 41 (1989).

Stancell, A. F. and A. T. Spencer, "Composite Permselective Membrane by Deposition of an Ultrathin Coating from a Plasma" J. Appl. Polym. Sci., **16**, 1505 (1972).

Stanley, M., "Thomas Graham and Gaseous Diffusion", Proc. 4th BOC Prestley Conf., Leeds Univ., (1986).

Stern, S. A., S. S. Kulkarni, and H. L. Frisch, "Test of a Free Volume Model of Gas Permeation Through Polymer Membranes", I. Pure CO_2, CH_4, C_2H_4 and C_3H_8 in Polyethlyene", J. Polym. Sci., Polym. Phys. ed., **21**, 467 (1983).

Stuart, M., "Tritium Content of Antractic Snow", Nature (London), **199**, 59 (1963).

Surface Chemistry and Physics", Plenum Press, N Y, 105, (1985).

Thenard, A., C. R. Hebd. Seances Acad. Sci., **78**,219 (1874).

Tibbitt, J. M., A. T. Bell and M. Shen, "Effects of Reaction Conditions on the Structure of Plasma Polymerized Ethylene", J. Macromol., A **11**, 139 (1977).

Tibbitt, J. M., M. Shen and A. T. Bell, "Structural Characterization of Plasma Polymerized Hydrocarbons", J. Macromol. Sci. Chem., **A 10**, 8, 1623 (1976).

Tkachuk, B. V. and A. I. Shustov, "Formation of Thin Polysiloxane Films in a Frequency Discharge", Khim. Vys. Energ., **9**, 468.(1972).

Vasile, M. J. and G. Smolinsky, "Organosilicon Films Formed by an rf [radio frequency] Polymerization Process", J. Electrochem. Soc., **119**, 451 (1972).

Vrentas, J. S. , and J. L. Duda, "Diffusion of Small Molecules in Amorphous Polymers", Mcromol., **9**, 785 (1976).

Vrentas, J. S. , and J. L. Duda, "Diffusion. In Encyclopedia of Polymer Science", ed. J. I. Kroschwitz, 2nd ed., **5**,. 36, (1986).

Vrentas, J. S. , and J. L. Duda, "Solvent and Temperature Effects on Diffusion in Polymer solvent Systems", J. Appl. Polym. Sci., **21**, 1715 (1977 b).

Wagner, C. D., W. M. Riggs, L.E. Davis, J. F. Moulder and G.E. Muilenberg, "Handbook of X-ray Photoelectron Spectroscopy", Perkin-Elmer Corporation, Eden Prairie, Minn, (1979).

Weisz, P. B., "Chemical Reactivity of CF_4 and C_2F_4 Induced by Electrical Discharge" J. Appl. Chem., **59**, 464 (1955).

Werner, U., "Some Technical and Economical Aspects of Gas Separation by Means of Membranes", Proc. 4th BOC Prestley Conf., Leeds Univ. (1986).

Wolff, J., K. E. Guido, and S. Hermann, "Porous Membranes", Ger. Offen., 45 pp., (1986).

Yamaguchi, T., ,N. Shinichi and K. Shoji, "Plasma-Graft Filling Polymerization : Preparation of a New Type of Pervaporation Membrane for Organic Liquid Mixtures", Macromolecules, **24** (20), 5522 (1991).

Yasuda, H., "Plasma Polymerization in an Electrodless Glow Discharge II Olefinic Monomers", Contemp. Top. Polym. Sci., **3**, 103 (1979).

Yasuda, H., "Plasma Polymerization", Academic Press Orlando, FL., (1984).

Yasuda, H., H. C. Marsh, E. S. Brandt and C. N. Reilley, "Preparation of Composite Reverse Osmosis Membranes by Plasma Polymerization of Organic Compounds IV. Influence of Plasma Polymer (Substrate) Interaction", J. Appl. Polym. Sci., **20**, 543 (1976).

Yasuda, H. and T. Hirotsu, "Disrribution of Polymer Deposition in Plasma Polymerization. II Effect of Reactor Design", J. Polym. Sci., **16**, 313 (1978).

Zisman, W. A. "Contact Angle-Wettability & Adhesion (R.F. Gould Ed.)", Am. Chem. Scoc., Washington, D.C.,P.1, (1964).

Appendix A

Computer Program

A.1 Resistance Program to Calculate Permeabilities and Resistances of Aniline Plasma Coated Membranes

A.1.1 Program Listing

```
C   Program name:-marie
C   Program name:-resi4
C    ********************
C   1. After the first assumption of alhpa3 = 0.0 and call the subroutine
C        the value of R3GAS1 is transfered to the subroutine in the 2nd
C        call and a second values are calculated for alpha3 and R3GAS1.
C   ------------------------------------------------------------------
C   The first half of this computer program calculates the unknows,
C   R12GAS1,R2GAS1,R3GAS1, and ALPHA3 using the modified resistance model.
C        ------------------------------------------------------------
C   The second half is a simulation program where the pore area, A3
C   and the lamination thickness is varied, while keeping R2, ALPHA2,
C   AREA2, L2, and ALPHA3 the same and calc. R3 by mult. by A3OLD/A3NEW.
C        ------------------------------------------------------------
C   INPUT EXPERIMENTAL Variables
C   ****************************
C 1-AREA1       = film area of the laminate (top layer) , m2
C 2-AREA2       = film area of the substrate membrane (bottom layer), m2
```

```
C 3-LAMTH      = thickness of top layer (laminate), m
C 4-PGAS1      = flux of 1st gas in the membrane before lamination, mol/s.m2.Pa
C 5-PGAS2      = flux of 2nd gas in the membrane before lamination, mol/s.m2.Pa
C 6-PLGAS1     = Permeability of 1st gas in laminated membrane , mol/s.m2.Pa
C 7-PLGAS2     = Permeability of 2nd gas in laminated membrane , mol/s.m2.Pa
C 8-LAMPG1     = intrin. permeability for 1st gas in top layer, mol.m/m2.s.Pa
C 9-LAMPG2     = intrin. permeability for 2nd gas in top layer, mol.m/m2.s.Pa
C 10-ALPHA2    = ratio of intrinsic permeabilities for (1st gas/2nd gas) in
C                the substrate membrane material (bottom layer).
C 11-GAS2      = is the other gas ie. N2, CO2, He, O2, CH4
C      ------------------------------------------------------------------
C  CALCULATED VALUES
C  *****************
C  1-A3          = area of aggregate pore in bottom layer (m2)
C  2-ALPHA3      = ratio of intrinsic permeability for (1st gas/2nd gas)
C                  in the pore
C      ------------------------------------------------------------------


      INTEGER ITMAX,N,NGAS,MM,I
      PARAMETER (N=2)
C     ------------------------------------------------------------------
      INTEGER K,NOUT
      REAL
      FCN,FNORM,R(N),XGUESS(N),AREA1,AREA2,LAMTH,PGAS2,PGAS1,
     1LAMPG1,LAMPG2,PLGAS1,PLGAS2,ALPHA2,RGAS1,ALPHA,ALPH1,RLGAS1,
     2   ALPHAL,R11GAS1,A3,X1,X2,ALPHA3,FCC,ERRREL,R3GAS1,
     3   Z3,RLH2A,L12,A32
      CHARACTER*40 NAME1,NAME2,NAME3,NAME4
      CHARACTER*78 TITLE,STITLE,UNLINE,DATSEP
C     ------------------------------------------------------------------
      COMMON /ONE/R11GAS1,RLGAS1,R3GAS1,ALPHA1,ALPHA2,ALPHAL
      EXTERNAL FCN,NEQNF,UMACH,FCC
```

```
C       ------------------------------------------------------------
        DATA AREA1,AREA2 / 9.62112E-4 , 9.62112E-4 /
C       ------------------------------------------------------------
        WRITE (6,100)
        READ  (5,101) NAME1,NAME2,NAME3
        OPEN(UNIT=1,NAME=NAME1,TYPE='OLD')
        OPEN(UNIT=2,NAME=NAME2,TYPE='UNKNOWN')
        OPEN(UNIT=3,NAME=NAME3,TYPE='UNKNOWN')
C       ------------------------------------------------------------
C                   First Half of the Program
C                   *************************
C       Assume :-
C       1. AREA2 = the area of the cell.
C       2. Thickness & intrinsic permeability of silicone rubber as
C          given by the manufacture.
C       For first approximation assume R3*alpha3 is equal to zero.
 9000   ALPHA3 = 0.0
        READ  (1,102,END=9999)
        DATSEP,TITLE,UNLINE,STITLE READ (1,*)
        XGUESS(1) , XGUESS(2) , AM1 , AM2 READ
        (1,*) PGAS1,PLGAS1,LAMPG1,LAMTH
        READ (1,*) PGAS2,PLGAS2,LAMPG2,ALPHA2
        WRITE (6,110)TITLE,STITLE,ALPHA2
C       ------------------------------------------------------------
        RGAS1     = 1.00/(PGAS1*AREA2)
        RLGAS1    = 1.00/(PLGAS1*AREA2)
        ALPHA     = PGAS1/PGAS2
        ALPHAL    = PLGAS1/PLGAS2
        ALPHA1    = LAMPG1/LAMPG2
C       ALPHA2  =  SUBPG1/SUBPG2
C       ALPHA3  = SQRT(AM2/AM1)
        R11GAS1  = LAMTH/(LAMPG1*AREA1)
        R11GAS2  = R11GAS1 * ALPHA1
```

```
      WRITE (2,150) TITLE,UNLINE,STITLE,XGUESS(1),XGUESS(2),LAMTH,
     1                PGAS1,PLGAS1,LAMPG1,PGAS2,PLGAS2,LAMPG2,
     2                ALPHA,ALPHAL,ALPHA1,ALPHA2
C     ---------------------------------------------------------------
C     ISML SUBROUTINE TO SOLVE NON LINEAR EQUATIONS
      ERRREL = 1.0
      ITMAX  = 50
      CALL UMACH(2,NOUT)
      CALL NEQNF(FCN,ERRREL,N,ITMAX,XGUESS,R,FNORM) R12GAS1 = R(1)
      R2GAS1  = R(2)
      R3GAS1  = (RGAS1*R2GAS1)/(R2GAS1-RGAS1)
      ALPHA3  = (ALPHA*RGAS1*ALPHA2*R2GAS1)/
     1          (ALPHA2*R3GAS1-ALPHA*RGAS1*R3GAS1)
      A3= LAMTH/(LAMPG1*R12GAS1)
      RGAS2= RGAS1*ALPHA
      RLGAS2  = RLGAS1*ALPHAL
      R11GAS2 = R11GAS1*ALPHA1
      R12GAS2 = R12GAS1*ALPHA1
      R2GAS2  = R2GAS1*ALPHA2
      R3GAS2  = R3GAS1*ALPHA3
C     ---------------------------------------------------------------
C     Using the values obtained from the first call in the second call
C=====================================================================
      Z3 = 0.0
  777 A3 = Z3
      ERRREL = 1.0
      ITMAX  = 50
      XGUESS(1) = R12GAS1
      XGUESS(2) = R2GAS1
      CALL UMACH(2,NOUT)
      CALL NEQNF(FCC,ERRREL,N,ITMAX,XGUESS,R,FNORM)
      R12GAS1 = R(1)
      R2GAS1  = R(2)
      R3GAS1  = (RGAS1*R2GAS1)/(R2GAS1 - RGAS1)
```

```
      ALPHA3  = (ALPHA*RGAS1*ALPHA2*R2GAS1) /
     1              (ALPHA2*R2GAS1*R3GAS1-ALPHA*RGAS1*R3GAS1)
      Z3= LAMTH/(LAMPG1*R12GAS1)
      MM= MM+1
      IF(ABS(Z3-A3).GT.ABS(0.00001*A3)) GO TO 777
      RGAS2= RGAS1*ALPHA
      RLGAS2  = RLGAS1*ALPHAL
      R11GAS2 = R11GAS1*ALPHA1
      R12GAS2 = R12GAS1*ALPHA1
      R2GAS2  = R2GAS1*ALPHA2
      R3GAS2  = R3GAS1*ALPHA3
C     ------------------------------------------------------------
      WRITE (2,160) MM,ALPHA3,RGAS1,RLGAS1,
     1   RGAS2,RLGAS2,R11GAS1,R12GAS1,R11GAS2,R12GAS2,R2GAS1,
     2   R2GAS2,R3GAS1,R3GAS2,A3,AREA1
      WRITE (3,161) ALPHA2,R2GAS1,R3GAS1,R2GAS2,R3GAS2
  161 FORMAT (F7.2,4E16.7)
C     ------------------------------------------------------------
C                       Second Half of the Program
C                       **************************
C     This part simulates membrane performance for varying substrate
C     porosities and lamination thickness.
      A32  = 0.1E-12
      DO 2000 II = 1,18
      A33= 2.50 * A32
      A32= A33
      R33H2= R3GAS1*(A3/A33)
      L12= 0.1E-6
      LAMTH= 0.0
      DO 1000 I = 1,30
      R11GAS1= LAMTH/(LAMPG1*AREA1)
      R12GAS1= LAMTH/(LAMPG1*A33)
      RLGAS1= ((R11GAS1+R2GAS1)*(R12GAS1+R33H2))/
     1              (R11GAS1+R12GAS1+R33H2)
```

```
      RLH2A= ((ALPHA1*R11GAS1+ALPHA2*R2GAS1)*
     1              (ALPHA1*R12GAS1+ALPHA3*R33H2))/
     1              (ALPHA1*R11GAS1+ALPHA2*R2GAS1+
     1              ALPHA1*R12GAS1+ALPHA3*R33H2)
      ALPHAL= RLH2A/RLGAS1
      PLGAS1= 1.0 / (RLGAS1*AREA2)
      LAMTH= L12*1.25
      L12= LAMTH
 1000 CONTINUE
 2000 CONTINUE
      GO TO 9000
C     ------------------------------------------------------------
  100 FORMAT (T2,'Enter 3 names :1.Input 2.Output 1 3.output 2 :-')
C 101 FORMAT (A40/A40/A40/A40)
  101 FORMAT (A40/A40/A40)
  103 FORMAT(A78)
  110 FORMAT(T1,A78/T1,A78/T2,'Assumed ALPHA2 = ',F6.2/T2,75('-'))
  115  FORMAT(/,2X,'A3',8X,'LAMTH',9X,'ALPHA L',4X,'H2 FLUX')
  120 FORMAT(/,1X,'AREA OF HOLE IN POLYETHERSULPHONE  = ',E11.4,' M2')
C     WRITE (2,150) TITLE,UNLINE,STITLE,XGUESS(1),XGUESS(2),LAMTH,
C    1              PGAS1,PLGAS1,LAMPG1,PGAS2,PLGAS2,LAMPG2,
C    2              ALPHA,ALPHAL,ALPHA1,ALPHA2
  150 FORMAT ('1',T2,A78/T2,A78/T2,A78//
     1 T2,'Initial Guess for R12GAS1 "XGUESS(1)"',T54,'=',E11.4/
     2 T2,'Initial Guess for R2GAS1   "XGUESS(2)"',T54,'=',E11.4/
     3 T2, 'Laminate Thickness (LAMTH)',T54,'=',E11.4,2X,'m'/
     4 T2,'1st gas permeability before lamination (PGAS1)',
     5  T54,'=',E11.4,2X,'mol/s.m2.Pa'/
     6 T2,'1st gas permeability After lamination (PLGAS1)',
     7  T54,'=',E11.4,2X,'mol/s.m2.Pa'/
     8 T2,'1st gas intrinsic permeability in laminate (LAMPG1)',
     9  T54,'=',E11.4,2X,'mol/s.m2.Pa'/
     1 T2,'2nd gas permeability before lamination (PGAS2)',
     2  T54,'=',E11.4,2X,'mol/s.m2.Pa'/
```

```
     3 T2,'2nd gas permeability After lamination (PLGAS2)',
     4  T54,'=',E11.4,2X,'mol/s.m2.Pa'/
     5 T2,'2nd gas intrinsic permeability in laminate (LAMPG2)',
     6  T54,'=',E11.4,2X,'mol/s.m2.Pa'//
     1 T21,'Permeability Ratios'/T21,19('*')/
     1 T2,'1st/2nd before lamination (ALPHA)' ,T54,'=',F11.3/
     3 T2,'1st/2nd after lamination (ALPHAL)',T54,'=',F11.3//
     1 T21,'Intrinsic Permeability Ratios'/T21,29('*')/
     5 T2,'1st/2nd in laminate (ALPHA1)',T54,'=',F11.3/
     7 T2,'1st/2nd in substrate (ALPHA2)',T54,'=',F11.3/
     9 T2,77('='))
160  FORMAT (T2,'Number of iterations to reach
     9 T2,'Calc. Permeability ratio in substrate pores (ALPHA3)',
     1  T54,'=',F11.3//
     1 T11,'Resistances in the Composite Membrane'/T11,37('*')//
     2 T2,'1st Gas Resistance before lamination (RGAS1)',
     3  T54,'=',E11.4,2X,'Pa.s/mol'/
     4 T2,'1st Gas Resistance After lamination (RLGAS1)',
     5  T54,'=',E11.4,2X,'Pa.s/mol'/
     6 T2,'2nd Gas Resistance before lamination (RGAS2)',
     7  T54,'=',E11.4,2X,'Pa.s/mol'/
     8 T2,'2nd Gas Resistance After lamination (RLGAS2)',
     9  T54,'=',E11.4,2X,'Pa.s/mol'/
     1 T2,'1st Gas Resistance (R11GAS1)',T54,'=',E11.4,2X,'Pa.s/mol'/
     2 T2,'1st Gas Resistance (R12GAS1)',T54,'=',E11.4,2X,'Pa.s/mol'/
     3 T2,'2nd Gas Resistance (R11GAS2)',T54,'=',E11.4,2X,'Pa.s/mol'/
     4 T2,'2nd Gas Resistance (R12GAS2)',T54,'=',E11.4,2X,'Pa.s/mol'/
     5 T2,'1st Gas Resistance (R2GAS1)',T54,'=',E11.4,2X,'Pa.s/mol'/
     6 T2,'2nd Gas Resistance (R2GAS2)',T54,'=',E11.4,2X,'Pa.s/mol'/
     7 T2,'1st Gas Resistance (R3GAS1)',T54,'=',E11.4,2X,'Pa.s/mol'/
     8 T2,'2nd Gas Resistance (R3GAS2)',T54,'=',E11.4,2X,'Pa.s/mol'/
     9 T2,'Area of hole in PES (A3)',T54,'=',E11.4,2X,'m2'/
     1 T2,'Area of Top Layer (AREA1)',T54,'=',E11.4,2X,'m2'/
     2 T2,75('='))
```

```
9999  STOP
      END
C
C     ****************************************************************
      SUBROUTINE FCN(R,F,N)
      INTEGER N
      REAL R(N),F(N)
      COMMON /ONE/R11GAS1,RLGAS1,R3GAS1,ALPHA1,ALPHA2,ALPHAL
      F(1) = RLGAS1 -
     1          ((R11GAS1+R(2))*R(1))/(R11GAS1+R(2)+R(1))
      F(2) = RLGAS1*ALPHAL -
     1          ((ALPHA1*R11GAS1+ALPHA2*R(2))*(ALPHA1*R(1)))/
     1          (ALPHA1*R11GAS1+ALPHA2*R(2)+ALPHA1*R(1))
      RETURN
      END
C
C     ****************************************************************
      SUBROUTINE FCC(R,F,N)
      INTEGER N
      REAL R(N),F(N)
      COMMON /ONE/R11GAS1,RLGAS1,R3GAS1,ALPHA1,ALPHA2,ALPHAL
      F(1) = RLGAS1 - ((R11GAS1+R(2))*(R(1)+R3GAS1))/
     1          (R11GAS1+R(2)+R(1)+R3GAS1)
      F(2) = RLGAS1*ALPHAL - ((ALPHA1*R11GAS1+ALPHA2*R(2))*
     1          (ALPHA1*R(1)+ALPHA3*R3GAS1))/
     1          (ALPHA1*R11GAS1+ALPHA2*R(2)+ALPHA1*R(1)+ALPHA3*R3GA1)
      RETURN
      END
```

A.1.2 Sample Data File

Membrane PES at a pressure of 758 KPa (Temp=35C)

Membrane is laminated with1.5 mil Silicon Rubber

CO_2 / CH4

1.0E14	1.0E15	44.0	16.0
4.6670E-07	2.7531E-09	9.04E-13	38.1E-06
3.6546E-07	1.1556E-10	2.68E-13	32.2

Membrane PES at a pressure of 758 KPa (Temp=30C)

Membrane is laminated with 1.5 mil Silicon Rubber

O_2 / N_2

1.0E12	1.0E10	32.0	28.0
4.1485E-07	3.7431E-10	1.67E-13	38.1E-06
4.2428E-07	1.1785E-10	8.37E-14	2.9222

A.1.3 Output Listing

Membrane PES at a pressure of 758 KPa (Temp=35C)

Membrane is laminated with 1.5 mil Silicon Rubber

CO_2 / CH_4

Initial Guess for R12GAS1 "XGUESS(1)"	=0.1000E+15
Initial Guess for R2GAS1 "XGUESS(2)"	=0.1000E+16
Laminate Thickness (LAMTH)	=0.3810E-04 m
1st gas permeability before lamination (PGAS1)	=0.4667E-06 mol/s.m^2.Pa
1st gas permeability After lamination (PLGAS1)	=0.2753E-08 mol/s.m^2.Pa
1st gas intrinsic permeability in laminate (LAMPG1)	=0.9040E-12 mol/s.m^2.Pa
2nd gas permeability before lamination (PGAS2)	=0.3655E-06 mol/s.m^2.Pa
2nd gas permeability After lamination (PLGAS2)	=0.1156E-09 mol/s.m^2.Pa
2nd gas intrinsic permeability in laminate (LAMPG2)	=0.2680E-12 mol/s.m^2.Pa

Permeability Ratios

1st/2nd before lamination (ALPHA)	=1.277
1st/2nd after lamination (ALPHAL)	=23.824

Intrinsic Permeability Ratios

1st/2nd in laminate (ALPHA1)	=3.373

1st/2nd in substrate (ALPHA2)	=32.200
Number of iterations to reach solution	=3
Calc. Permeability ratio in substrate pores (ALPHA3)	=1.277

Resistances in the Composite Membrane

1st Gas Resistance before lamination (RGAS1)	=0.2227E+10 Pa.s/mol
1st Gas Resistance After lamination (RLGAS1)	=0.3775E+12 Pa.s/mol
2nd Gas Resistance before lamination (RGAS2)	=0.2844E+10 Pa.s/mol
2nd Gas Resistance After lamination (RLGAS2)	=0.8994E+13 Pa.s/mol
1st Gas Resistance (R11GAS1)	=0.4381E+11 Pa.s/mol
1st Gas Resistance (R12GAS1)	=0.2502E+13 Pa.s/mol
2nd Gas Resistance (R11GAS2)	=0.1478E+12 Pa.s/mol
2nd Gas Resistance (R12GAS2)	=0.8440E+13 Pa.s/mol
1st Gas Resistance (R2GAS1)	=0.1957E+16 Pa.s/mol
2nd Gas Resistance (R2GAS2)	=0.6302E+17 Pa.s/mol
1st Gas Resistance (R3GAS1)	=0.2227E+10 Pa.s/mol
2nd Gas Resistance (R3GAS2)	=0.2844E+10 Pa.s/mol
Area of hole in PES (A3)	=0.1684E-04 m^2
Area of Top Layer (AREA1)	=0.9621E-03 m^2

Membrane PES at a pressure of 758 KPa (Temp=30C)

Membrane is laminated with 1.5 mil Silicon Rubber

O_2 / N_2

Initial Guess for R12GAS1 "XGUESS(1)"	=0.1000E+13	
Initial Guess for R2GAS1 "XGUESS(2)"	=0.1000E+11	
Laminate Thickness (LAMTH)	=0.3810E-04	m
1st gas permeability before lamination (PGAS1)	=0.4149E-06	mol/s.m^2.Pa
1st gas permeability After lamination (PLGAS1)	=0.3743E-09	mol/s.m^2.Pa
1st gas intrinsic permeability in laminate (LAMPG1)	=0.1670E-12	mol/s.m^2.Pa
2nd gas permeability before lamination (PGAS2)	=0.4243E-06	mol/s.m^2.Pa
2nd gas permeability After lamination (PLGAS2)	=0.1178E-09	mol/s.m^2.Pa
2nd gas intrinsic permeability in laminate (LAMPG2)	=0.8370E-13	mol/s.m^2.Pa

Permeability Ratios

1st/2nd before lamination (ALPHA	=0.978
1st/2nd after lamination (ALPHAL)	=3.176

Intrinsic Permeability Ratios

1st/2nd in laminate (ALPHA1)	=1.995
1st/2nd in substrate (ALPHA2)	=3.2
Number of iterations to reach solution	=5

Calc. Permeability ratio in substrate pores (ALPHA3)	=0.977

Resistances in the Composite Membrane

1st Gas Resistance before lamination (RGAS1)	=0.2505E+10 Pa.s/mol
1st Gas Resistance After lamination (RLGAS1)	=0.2777E+13 Pa.s/mol
2nd Gas Resistance before lamination (RGAS2)	=0.2450E+10 Pa.s/mol
2nd Gas Resistance After lamination (RLGAS2)	=0.8820E+13 Pa.s/mol
1st Gas Resistance (R11GAS1)	=0.2371E+12 Pa.s/mol
1st Gas Resistance (R12GAS1)	=0.1491E+19 Pa.s/mol
2nd Gas Resistance (R11GAS2)	=0.4731E+12 Pa.s/mol
2nd Gas Resistance (R12GAS2)	=0.2975E+19 Pa.s/mol
1st Gas Resistance (R2GAS1)	=0.2823E+13 Pa.s/mol
2nd Gas Resistance (R2GAS2)	=0.8249E+13 Pa.s/mol
1st Gas Resistance (R3GAS1)	=0.2508E+10 Pa.s/mol
2nd Gas Resistance (R3GAS2)	=0.2450E+10 Pa.s/mol
Area of hole in PES (A3)	=0.1530E-09 m^2
Area of Top Layer (AREA1)	=0.9621E-03 m^2